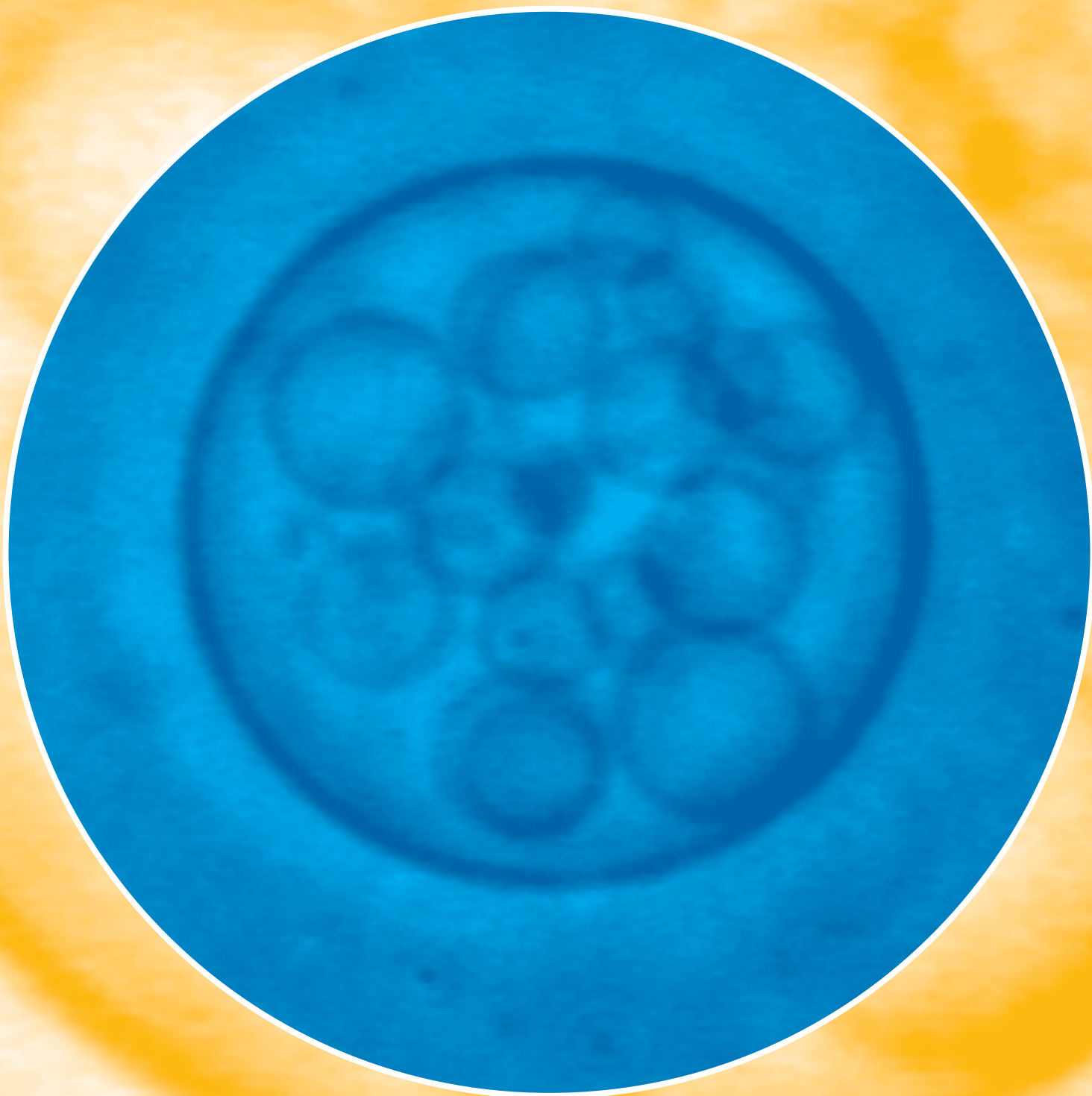THEORY

Research in the Theory Department

Es gibt nichts Praktischeres als eine gute Theorie

Immanuel Kant

Structure of the Theory Department

The researchers and doctoral students of the Theory Department form one experimental and seven theoretical research teams. Each of these teams consists of the team leader and several students. The team leaders are:

· Rumiana Dimova (experiment, membranes and vesicles).
· Thomas Gruhn (theory, membranes and vesicles);
· Jan Kierfeld (theory, polymers and filaments);
· Stefan Klumpp (theory, transport by molecular motors);
· Ulrich Schwarz (theory, membranes and cells) (until 2005);
· Christian Seidel (theory, polymers and polyelectrolytes);
· Julian Shillcock (theory, supramolecular modelling);
· Thomas Weikl (theory, proteins and membranes).

The Theory Department is responsible for the International Max Planck Research School and for the European Early Stage Training Network in which three departments of the MPI participate. The management of these networks is done by Angelo Valleriani.

Research in the Theory Department is focused on fundamental aspects of colloids and interfaces. In most cases, we study biomimetic model systems which are inspired by the nanostructures found in biological systems. Two examples are bilayer membranes with several components and active transport by molecular motors. In addition, some work has been done to directly address the complexity of biological systems. Two examples are the kinetics of protein folding and the elastic interactions of cells.

The conceptual framework for the understanding of these systems and their cooperative behavior is provided by *statistical physics* which includes thermodynamics, statistical mechanics, and stochastic processes. Some fundamental aspects of statistical physics such as irreversible processes and networks have also been pursued.

In the following three subsections, the research within the Theory Department is described in more detail in terms of the underlying systems which exhibit a hierarchy of structural levels, the generic phenomena found in these systems, and the methods used to study them.

Systems

First, one can emphasize the various systems which are studied in the department. If one looks at these systems bottom-up, i.e., from small to large scales, one can distinguish several levels of bionano systems as shown in **Fig. 1**.
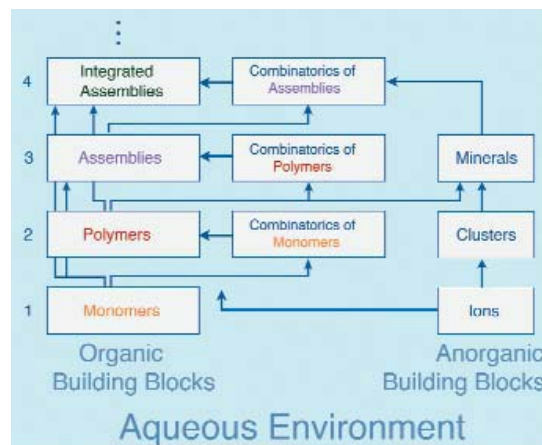

Fig. 1: Hierarchy of bionano systems, i.e., of biological and biomimetic systems in the colloidal regime between nanometers and micrometers. The assembly pathway on the left proceeds from small molecules or monomers to integrated assemblies, i.e., to 'assemblies of assemblies' that may differ in their architecture. The assembly pathway on the right leads to small mineral particles that are stabilized by adsorbed polymers.
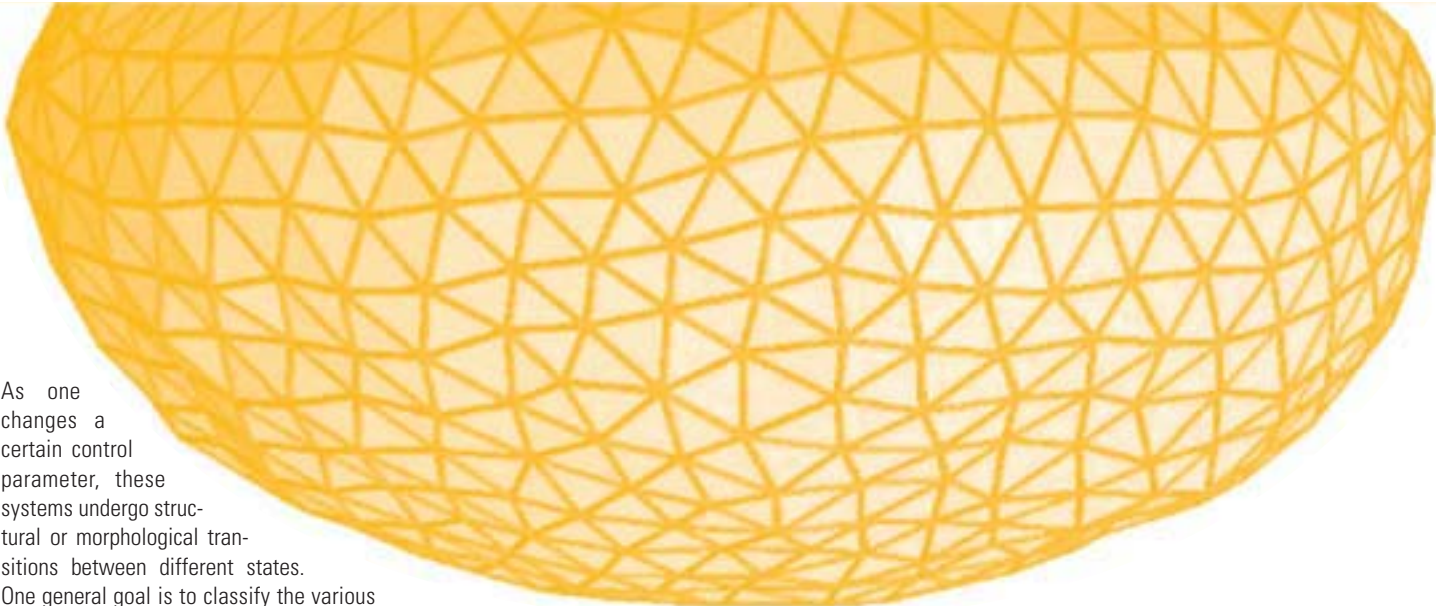
During the last two years, research on biomimetic systems has been focussed on the levels of polymers (polyelectrolytes, semi-flexible polymers, mesoscopic rods), assemblies (cytoskeletal filaments, bilayer membranes), and integrated assemblies consisting, e.g., of filaments, motors, and cargo particles such as vesicles. Research on biological systems addressed the level of polymers in the context of protein folding and the level of whole cells which lies above those shown in **Fig. 1**.

If one looks at these systems top-down, i.e., from large to small scales, one encounters the problem of restricted geometries or confining walls and interfaces. One topic in this latter research area which has been studied in some detail were liquids at chemically and topographically structured surfaces.

Phenomena

At each level shown in **Fig. 1**, one encounters a variety of cooperative phenomena. These systems contain flexible or soft components that undergo thermally excited fluctuations corresponding to cooperative Brownian motion because the ambient temperature corresponds to liquid water. One would like to determine both, the typical states or morphologies attained by these systems and their fluctuation spectrum. In addition, these fluctuations lead to entropically induced forces which compete with the direct molecular forces.
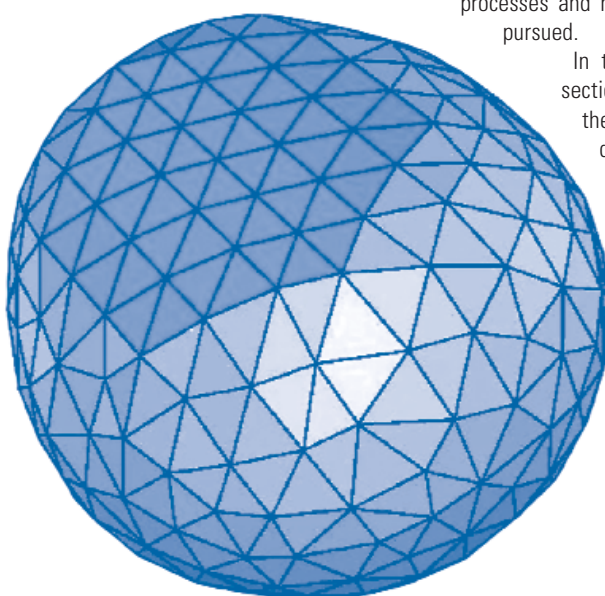
As one changes a certain control parameter, these systems undergo structural or morphological transitions between different states. One general goal is to classify the various possible states and their transitions. This classification leads to "state", "morphology", or "phase" diagrams which describe the system's behavior in a global manner.

One structural transition which has been studied in the Theory Department during the last two years, both experimentally and theoretically, is the fusion of bilayer membranes and vesicles. In the experiments, the fusion was induced by the addition of multivalent ions which act to crosslink certain membrane-anchored molecules. In the simulations, the fusion was controlled by the initial tensions within the membranes. At present, the length scales accessible to experiments and simulations are still rather different whereas the time scales now begin to have some overlap.

Membrane fusion starts from an adhering state and is completed when the fusion pore has been formed. Such a fusion event represents an irreversible relaxation or "downhill" process that proceeds from an initial state out of equilibrium towards another more stable state.

In order to reverse this process, one would need to involve a molecular motor that can break the neck of the fusion pore again. Such a motor must be able to couple the fission of the fusion pore, which represents an endergonic "uphill" process, to another process that represents an exergonic "down-hill" process. This type of coupling provides the basic mechanism for all active processes in biological systems.

Active biomimetic processes have now become a main focus of the Theory Department.

One important example is the transport by molecular motors. In this context, we have studied a variety of cooperative motor phenomena: build-up of traffic jams of motors; active structure formation leading to steady states with spatially non-uniform density and current patterns; and active phase transitions between different steady states far from equilibrium. A particularly simple active phase transition with spontaneous symmetry breaking is predicted to occur in systems with two species of motor particles which walk on the filaments in opposite directions.

Current projects on active processes include: effect of disordered filaments and regulatory proteins on motor transport; active force generation by polymerization; cooperative behavior of filaments on motor covered substrates; adhesion of membranes with active stickers.

In addition, the Theory Department coordinates a new European network (STREP) on "Active Biomimetic Systems".

Methods

The theoretical work starts with the definition of a certain model which (i) is amenable to systematic theoretical analysis and (ii) captures the essential features of the real system and its behavior. New models which have been introduced in the Theory Department include: semi-flexible harmonic chains for filaments; coarse-grained molecular models for bilayer membranes; lattice models for membranes with adhesion molecules; geometric models for membranes with lateral domains; and lattice models for transport by molecular motors.

These theoretical models are then studied using the analytical tools of theoretical physics and a variety of numerical algorithms. The analytical tools include dimensional analysis, scaling arguments, molecular field or self-consistent theories, perturbation theories, and field-theoretic methods such as renormalization. The numerical methods include the application of mathematical software packages such as Mathematica or Maple as well as special algorithms such as, e.g., the Surface Evolver for the calculation of constant mean curvature surfaces.

Three types of computer simulations are applied and further developed: Molecular Dynamics, Dissipative Particle Dynamics, and Monte Carlo methods. Molecular Dynamics is applied to particle based models of supramolecular assemblies; Dissipative Particle Dynamics, which is a relatively new simulation algorithm, is useful in order to extend the Molecular Dynamics Studies towards much larger systems and longer time scales; Monte Carlo methods are used in order to simulate even larger mesoscopic systems such as filaments and membranes up to a linear size of hundreds of nanometers.

The experimental work is carried out in our membrane lab which is equipped with calorimetry, optical microscopy, micropipettes, and optical tweezers. An advanced confocal microscope is currently installed that will be available to all four departments of the MPI.

Additional information about research in the Theory Department is avalaible at *www.mpikg.mpg.de/th/*.

Reinhard Lipowsky
Director of the Theory Department

103
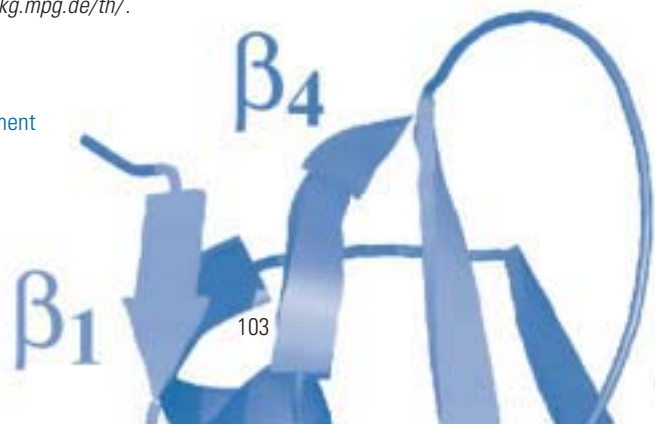
Wetting Morphologies at Structured Surfaces

Reinhard Lipowsky 11.11.1953
1978: Diploma, Physics,
Thesis with Heinz Horner on
turbulence (University of Heidelberg)
1982: PhD (Dr. rer. nat.), Physics
(University of Munich)
Thesis with Herbert Wagner
on surface phase transitions
1979-1984: Teaching Associate with
Herbert Wagner (University of Munich)
1984-1986: Research Associate with
Michael E. Fisher (Cornell University)
1986-1988: Research Associate with
Heiner Müller-Krumbhaar (FZ Jülich)
1987: Habilitation, Theoretical Physics
(University of Munich)
Thesis: Critical behavior of interfaces:
Wetting, surface melting and related
phenomena
1989-1990: Associate Professorship
(University of Munich)
1990-1993: Full Professorship
(University of Cologne), Director of
the Division "Theory II" (FZ Jülich)
Since Nov 1993: Director
(Max Planck Institute of Colloids
and Interfaces, Potsdam)

Many experimental methods have been developed by which one can prepare chemically and/or topographically structured substrates. If one deposits a certain amount of liquid on such a substrate, one experimentally observes a large variety of wetting morphologies.

Some years ago, we started to classify the possible morphologies at *chemically* structured surfaces theoretically. We discovered that these surfaces lead to *morphological wetting transitions* at which the wetting layer changes its shape in a characteristic and typically abrupt manner [1, 2]. We extended this work (i) to liquid channels or filaments with freely moving endcaps which leads to a morphology diagram with a line of discontinuous transitions that ends in a critical point [3], see biannual report 2002+2003, (ii) to nucleation at circular surface domains which is characterized by an activation free energy with two maxima [4], (iii) to vesicle adhesion at striped surface domains [5], and (iv) to a general stability analysis of these morphologies [6].

In the context of nonplanar substrates, we first studied chemically heterogeneous and *topographically* rough surfaces for which we derived the general functional relationship between contact angle, interfacial tensions, and line tension [7]. More recently, we considered topographically structured surfaces which contain surface channels (or grooves) and obtained a complete classification for the corresponding wetting morphologies [8]. The following contribution will focus on this latter work.

Open Systems for Micro- and Nanofluidics

An obvious prerequisite for "labs-on-a-chip" miniaturized labs are appropriate micro-compartments for the confinement of very small amounts of liquids and chemical reagents. Like the test-tubes in macroscopic laboratories, these micro-compartments should have some basic properties: They should have a well-defined geometry by which one can measure the precise amount of liquid contained in them; they should be able to confine *variable* amounts of liquid; and they should be accessible in such a way that one can add and extract liquid in a convenient manner.

An appealing design principle for such microcompartments is based on open and, thus, directly accessible surface channels which can be fabricated on solid substrates using available photolithographic methods. The simplest channel geometry that can be produced in this way corresponds to channels with a rectangular cross section. The width and depth of these channels can be varied between a hundred nanometers and a couple of micrometers.

Classification of Wetting Morphologies

As shown in our recent study [8], liquids at surface channels can attain a large variety of different wetting morphologies including localized droplets, extended filaments, and thin wedges at the lower channel corners. Examples for these morphologies as observed by atomic (or scanning) force microscopy (AFM) are shown in **Fig. 1**.
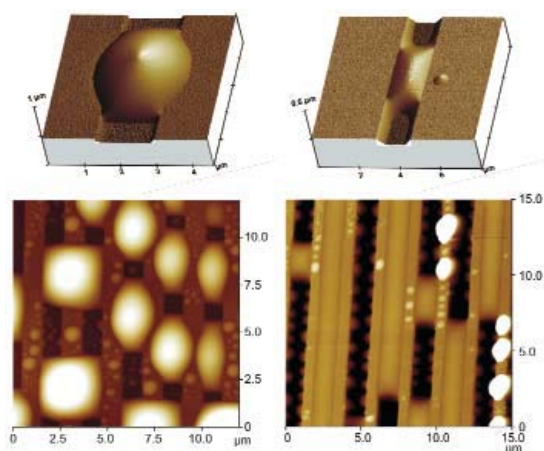

Fig. 1: Atomic (or scanning) force microscopy images of liquid morphologies on silicon substrates with rectangular surface channels which have a width of about one micrometer. On the left, the liquid does not enter the channels but forms large lemon-shaped droplets overlying the channels (dark stripes). On the right, the liquid enters the channels and forms extended filaments separated by essentially empty channel segments (dark stripes). In the bottom row, one sees several parallel surface channels in both images; in the top row, there is only one such channel with a single droplet (left) or filament (right). Close inspection of the upper right image reveals (i) that this filament is connected to thin wedges along the lower channel corners and (ii) that the contact line bounding the meniscus of the filament is pinned to the upper channel edges.

When the AFM experiments were first performed, it was not known how to produce a certain liquid morphology since there was no systematic theory for the dependence of this morphology on the materials properties and on the channel design. Such a theory has now been developed. Our theory addresses the strong capillary forces between substrate material and liquid and takes the 'freedom' of contact angles at pinned contact lines into account. Such a contact line is visible in the upper right image in **Fig. 1**. For this contact line, which is pinned along the channel edges, the contact angle θ_p is not determined by the classical Young equation but can vary over the range

$$\theta \leq \theta_p \leq \theta + \pi/2 \qquad (1)$$

for a surface channel with rectangular cross section where θ denotes the contact angle on all planar segments of the substrate surface (taken to be chemically homogeneous). An analogous 'freedom' is also found for those contact lines that are pinned to the boundaries of chemically defined surface domains as first emphasized and explored in our previous work [1].

The classification described in [8] is based (i) on general considerations such as the relation given by (1), (ii) on analytical shape calculations which are feasible for relatively simple morphologies such as liquid filaments with constant cross section, see **Fig. 2**, and (iii) on numerical minimization of the liquid's free energy which leads to constant mean curvature surfaces. A surprising prediction of our theory is that the experimentally observed polymorphism of the wetting liquid

depends only on two parameters: (i) the aspect ratio X of the channel geometry, i.e., the ratio of the channel depth to the channel width; and (ii) the contact angle θ which characterizes the interaction between substrate material and liquid.

The corresponding morphology diagram, which is displayed in **Fig. 3**, represents a complete classification of all possible wetting morphologies.

Inspection of this figure shows that one has to distinguish seven different liquid morphologies which involve localized droplets (D), extended filaments (F), and thin wedges (W) at the lower channel corners.

For microfluidics applications, the most important morphology regime is (F$^-$) which corresponds to stable filaments. Since this regime covers a relatively small region of the morphology diagram, see **Fig. 3**, it can only be obtained if one carefully matches the channel geometry described by its aspect ratio X with the substrate wettability as described by the contact angle θ.
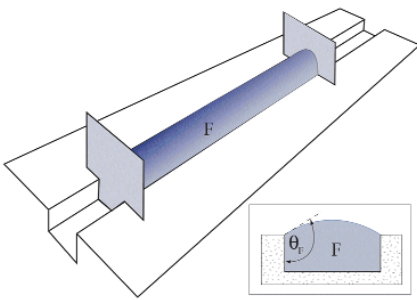

Fig. 2: Liquid filament (F$^+$) with positive Laplace pressure, i.e., with a meniscus that is curved upwards away from the substrate. The filament is located within the rectangular surface channel and is "sandwiched" between two pistons which provide walls orthogonal to the long axis of the filament. The contact angle at these walls is π/2 which ensures that the filament has constant cross-section and is bounded by a cylindrical meniscus. In mechanical equilibrium, the total force exerted by the filament onto each piston must vanish. The inset shows the filament cross section and the associated filament angle $\theta_p = \theta_F$ which is uniquely determined by the aspect ratio X of the surface channel and the contact angle θ of the substrate material.
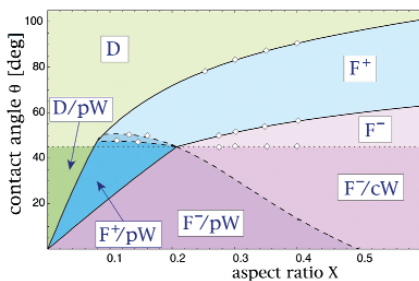

Fig. 3: Morphology diagram as a function of the aspect ratio X of the channel and the contact angle θ which characterizes the interaction between substrate material and liquid. This diagram contains seven different morphology regimes which involve localized droplets (D), extended filaments (F), and thin wedges (W) in the lower channel corners. The diagram represents a complete classification of all possible wetting morphologies and should be universal, i.e., should apply to other liquids and substrate materials as well.

Perspectives

One relatively simple application of the morphology diagram shown in **Fig. 3** is obtained if the system is designed in such a way that one can vary or switch the contact angle in a controlled fashion. One such method is provided by electrowetting; alternative methods, which have been recently developed, are substrate surfaces covered by molecular monolayers that can be switched by light, temperature, or electric potential. If one varies the contact angle by one of these methods, the system moves in the morphology diagram parallel to the vertical axis. It can then cross the boundary between the two morphology regimes (F$^-$) and (F$^+$). This transition leads to a controlled variation in the length of the liquid filament: these filaments enter the surface channels with decreasing contact angle but recede from these channels with increasing contact angle as has been demonstrated by electrowetting experiments.

The theory underlying the morphology diagram in **Fig. 3** predicts that this diagram is rather universal and applies to many different systems. The experiments described in **[8]** use a polymeric liquid that freezes quickly and can then be scanned directly with the tip of an atomic force microsope.

The morphology diagram should also apply to other liquids and other substrate materials. It should also remain valid if one further shrinks the surface channels and, in this way, moves deeper into the nanoregime. As one reaches a channel width of about 30 nanometer, one theoretically expects new effects arising from the line tension of the contact line, but such nanochannels remain to be studied experimentally.

R. Lipowsky, P. Blecua, M. Brinkmann, R. Dimova, J. Kierfeld
lipowsky@mpikg.mpg.de

References:
[1] Lenz, P. and Lipowsky, R.: Morphological transitions of wetting layers on structured surfaces. Phys. Rev. Lett. **80**, 1920-1923 (1998). Gau, H., Herminghaus, S., Lenz, P. and Lipowsky, R.: Liquid Morphologies on Structured Surfaces: From Microchannels to Microchips. Science **283**, 46-49 (1999).
[2] Lipowsky, R.: Morphological wetting transitions at chemically structured surfaces. Curr. Opin. Colloid and Interface Sci. **6**, 40-48 (2001).
[3] Brinkmann, M. and Lipowsky, R.: Wetting morphologies on substrates with striped surface domains. J. Appl. Phys. **92**, 4296-4306 (2002).
[4] Valencia, A. and Lipowsky, R.: Nucleation through a double barrier for a chemically patterned substrate. Langmuir **20**, 1986-1996 (2004).
[5] Lipowsky, R., Brinkmann, M., Dimova, R., Franke, T., Kierfeld, J. and Zhang, X.: Droplets, Bubbles, and Vesicles at Chemically Structured Surfaces. J. Phys. Cond. Mat. (in press).
[6] Brinkmann, M., Kierfeld, J. and Lipowsky, R.: A general stability criterion for droplets on structured substrates. J. Phys. A **37**, 11547-11573 (2004).
[7] Swain, P. and Lipowsky, R.: Contact angles on structured surfaces: a new look at Cassie's and Wenzel's laws. Langmuir **14**, 6772-6780 (1998). Lipowsky, R., Lenz, P. and Swain, P.: Wetting and Dewetting of Structured or Imprinted Surfaces. Colloids and Surfaces A, **161**, 3-22 (2000).
[8] Seemann, R., Brinkmann, M., Kramer, E. J., Lange, F. F. and Lipowsky, R.: Wetting morphologies at microstructured surfaces. Proc. Nat. Sci. USA, **102**, 1848-1852, 2005; see also Science **307**, 9095 (2005).

MEMBRANES AND VESICLES

Mesoscopic Simulations of Complex Nanostructures and Processes

Julian Charles Shillcock 18.10.1960
1982: B.Sc (Hons), Physics
(Kings College London)
1985: M.Sc, Nuclear Physics
(Simon Fraser University, Canada)
Thesis: Hanbury-Brown Twiss Effect
in Heavy-Ion Collisions
1986-1990: Research Scientist
(British Aerospace, Space Systems
Division, U.K.)
1995: PhD, Biophysics
(Simon Fraser University, Canada)
Thesis: Elastic Properties of Fluid and
Polymerised Membranes under Stress
1995-1997: Postdoc
(Max Planck Institute of Colloids
and Interfaces, Potsdam)
1998-1999: Senior Scientist (Molecular
Simulations Inc., Cambridge, U.K.)
1999-2003: Group Leader
(Max Planck Institute of Colloids
and Interfaces, Potsdam)

The traditional boundaries between the scientific disciplines of Physics, Chemistry and Biology are being rapidly eroded at the nanoscale. This is a new development largely because at the macroscale it is clear that there is a vast difference between whole organisms, even ones as small as an amoeba, and the atoms and molecules of chemistry and physics. As one probes down to smaller length scales, however, these distinctions become increasingly artificial. Progress in electron microscopy, fluorescence techniques and micromanipulation have pushed the experimental resolution of investigations of the protein and lipid components of cells to smaller and smaller length scales while, simultaneously, novel computer simulation techniques are starting to reveal structure above the 50 nm and 100 ns marks. However, the intermediate region, between 100 nm and 1 micron, and 100 ns and 100 microseconds, is still partially obscure: the so-called twilight zone [1].

In this project, we are using a mesoscopic simulation technique, Dissipative Particle Dynamics (DPD), to probe this twilight zone. We hope to predict the properties of "smart" self-assembled materials, such as amphiphilic membranes and actin filaments, from a knowledge of their constituents (see **Fig. 1**); and to reveal details of biophysical processes, such as vesicle fusion, unobtainable from continuum theoretical models and difficult to quantify from experiment. In collaboration with a group at University of Pennsylvania, we have also started to perform a systematic comparison of DPD simulations with more traditional Molecular Dynamics (MD) simulations using diblock copolymers as a target system of topical interest.
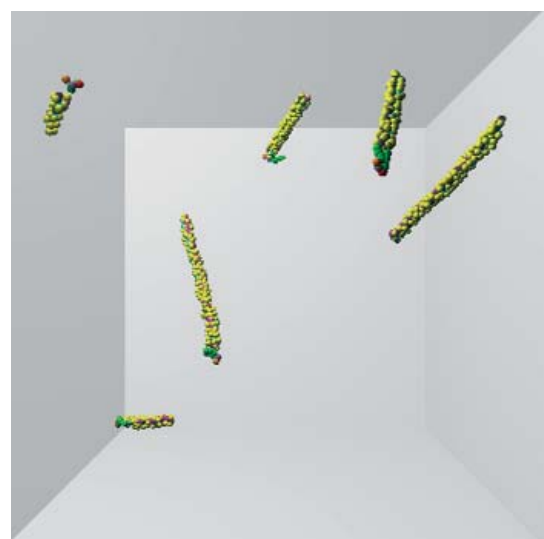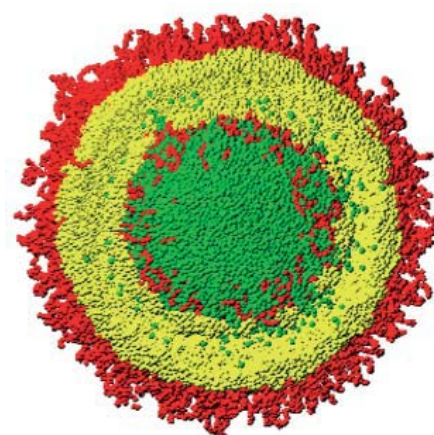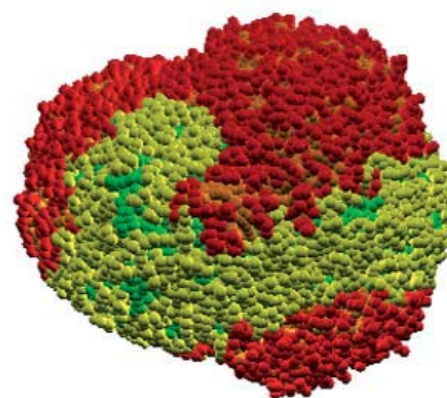

Fig. 1: Illustrations of a two-component vesicle (Illya, PhD Thesis, 2004), a 40 nm polymersome (Ortiz et al., 2005), and growing actin filaments (Shillcock and Lipowsky, in progress). Note that the images are not to the same scale.

Amphiphilic membranes are ubiquitous in nature, and have important technological applications as well. Ms Gregoria Illya, who graduated in December 2004, has used DPD simulations to map out the dependence of amphiphilic membrane structural properties (area per molecule, thickness, density profile) and material properties (lateral stress profile, area stretch modulus and bending modulus) for a homologous series of amphiphiles [2]. Mixed membranes containing two types of amphiphile with different tail lengths have also been investigated. For amphiphiles that mix ideally, the membrane area stretch modulus is a non-monotonic function of the composition, in agreement with mean field theories. Amphiphiles that tend to phase separate in the membrane form domains whose shape changes from small circular patches, through stripes, to inverted circular patches as the concentration of the close-packed amphiphile is increased.

Diblock copolymers form closed vesicles called Polymersomes. These systems are of great interest as drug delivery vehicles, amongst other applications, because they are more robust than lipid vesicles, and their material properties can be systematically varied depending on the molecular details of their constituents [3]. Together with the group of Prof. Dennis Discher at University of Pennsylvania, we have used DPD simulations to study the properties of polymersomes. We have calibrated the parameters of our DPD diblock model using the Penn group's all-atom and coarse-grained MD simulations. The results are currently being submitted [4], and show that the common assumption in DPD simulations to date that all beads have a common density must be abandoned if the physical properties of the diblock model are to match those of the corresponding experimental system.

The second part of our work is the study of dynamic processes on a mesoscopic scale. As a model system, the fusion of a 28 nm vesicle to a 50 x 50 nm^2 patch has been simulated for up to 2 microseconds using two protocols. The first places the vesicle and membrane patch under initial tensions, and lets the system evolve without further interference. The second protocol places an initially relaxed vesicle next to a relaxed planar membrane patch, and uses a sequence of bending and stretching forces, mimicking the actions of the fusion proteins, to drive the fusion process. The tension-controlled fusion depends sensitively on the size of the membrane patch to which the vesicle fuses and, for the 50 nm patch used here, predicts a pore formation time (measured from the time of first contact between vesicle and planar membrane) of 200-300 ns. This is far below the current experimental resolution of fusion, showing that coarse-grained simulations can already explore regimes that are not yet experimentally characterised. These results have recently been accepted for publication [5]. The fusion of membranes with novel molecular architectures and material properties is being extended by a recently-arrived post-doctoral fellow, Dr Lianghui Gao, and a new PhD student, Ms Andrea Grafmüller. The second protocol is still being developed, and we aim to compare the forces required to drive fusion with experimentally-measured forces [6]) in order to make predictions about the minimal molecular machinery that can produce reliable vesicle fusion.

Finally, we are using DPD to simulate the self-assembly of actin filaments. Within the framework of a Human Frontier Science Project grant, we are exploring a model of Formin-mediated filament assembly. Formin is a protein that sequentially adds actin monomers to a growing filament while maintaining a constant "grip" on the filament. The monomers bind using non-covalent forces; the filaments are polar, with different growth/shrinkage rates at each end; and the filament stiffness is sensitive to the nature of the bonds holding monomers together. This system has been the subject of recent experimental work [7], and we hope to measure the force exerted by a formin molecule bound to a small bead on a growing filament.

J. C. Shillcock, L. Gao, A. Grafmüller, G. Illya, R. Lipowsky
Julian.Shillcock@mpikg.mpg.de

References:
[1] Lipowsky, R.: Pictures from the twilight zone. New and Views, Nature Materials **3**, 589-591 (2004).
[2] Illya, G., Lipowsky, R., and Shillcock, J.C.: Effect of chain length and asymmetry on membrane material properties. Submitted (2005).
[3] Discher, D.E. and Eisenberg, A.: Polymer vesicles. Science **297**, 967-973 (2002).
[4] Ortiz, V., Nielsen, S.O., Discher, D.E, Klein, M.L., Lipowsky, R. and Shillcock, J.C.: Dissipative particle dynamics simulations of polymersomes. (in progress 2005).
[5] Shillcock, J.C. and Lipowsky, R.: Tension-induced fusion of membranes and vesicles. Nature Materials, (accepted Dec. 2004).
[6] Yersin, A. et al.: Interactions between synaptic vesicle fusion proteins explored by atomic force microscopy. PNAS. **100**, 8736-8741 (2003).
[7] Higashida, C. et al.: Actin polymerization-driven molecular movement of mDia1 in living cells. Science **303**, 2007-2010 (2004).

Properties of Thermally Fluctuating Vesicles

Thomas Gruhn 10.06.1969
1995: Diploma, Physics
(Technische Universität Berlin)
Thesis: Monte-Carlo-Untersuchungen
der Ausrichtung nematischer Flüssig-
kristalle (A Monte Carlo study of the
alignment in nematic liquid crystals)
1998: PhD, Physics (Institut für
Theoretische Physik, TU Berlin)
Thesis: Substrate-induced order in
confined molecularly thin liquid-
crystalline films
1999: R&D Project
(Siemens AG, Berlin)
2000: Postdoc
(University of Massachusetts, USA)
2001: Group Leader
(Max Planck Institute for Colloids
and Interfaces, Potsdam)

Properties of Thermally Fluctuating Vesicles

All forms of life are based on the principle of screening small regions from the chemical conditions of the surrounding. Lipid membranes are an excellent material for this purpose. Vesicles basically consist of a closed fluid membrane shell, which is impermeable for most larger molecules. On the other hand, lipid membranes can be penetrated by water molecules and due to their fluidity they can adapt to steric constraints imposed by the environment [1]. The research on vesicles provides much insight into the behavior of living cells. Many mechanical and chemical cell properties can be mimicked using lipid membranes and vesicles. An effect that depends on chemical and mechanical properties is the formation of solid domains in a fluid membrane of a vesicle [2]. We investigate the stability of different domain shapes by a comparison of their free energies **Fig. 1**.
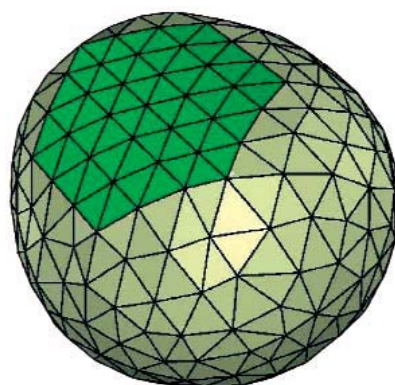

Fig. 1: Model of a vesicle with a solid domain.

Vesicles are not only important to mimic cell properties they can also be used as transport vehicles for the specific application of medically active agents. Not only do they protect their load in the inside from immune reactions of the body, there is also evidence that they can squeeze through small skin pores [3]. An investigation of this effect is discussed in the last paragraph.

At first, some more basic aspects are discussed, namely the spontaneous asphericity of free vesicles and a method to measure the binding free energy of vesicles adhering to a substrate.

Basic Properties of Vesicles

The deformation of lipid membranes results in a change of the bending energy. In the simplest case the membrane has no spontaneous curvature, which means, it is preferentially flat. The bending energy is proportional to the bending rigidity κ.

In the presence of larger molecules that cannot permeate through the membrane, an osmotic pressure acts on the vesicle. These molecules are therefore called "osmotically active". The pressure vanishes if the vesicle reaches a volume where the concentration of osmotically active molecules in- and outside the vesicle is equal. In this way, the volume of the vesicle can be controlled by the external molecular concentration.

Free Fluid Vesicles are not Exactly Spherical

We consider a vesicle with no spontaneous curvature in the absence of osmotically active molecules. For very low temperatures, the vesicle assumes the shape with the lowest configurational energy, which is a sphere. For finite temperatures it is often assumed that the vesicle performs small fluctuations around the preferred spherical shape. This is, however, not true. In Monte Carlo simulations we have calculated the free energy F(d) as a function of the order parameter d, which is a measure for the asphericity of the vesicle [4]. The parameter d is positive for prolate vesicle shapes, negative for oblate shapes, and zero for sphere-like vesicles. In **Fig. 2** a typical plot of F(d) is shown, which has two minima at about d=+0.1 and d=-0.1, which are the preferred degrees of asphericity. At d=0 there is a distinct maximum, which means that the vesicle is preferentially aspherical. A similar behavior still exists for a small osmotic excess pressure inside the vesicle, which generally stabilizes the sphere shape. For higher excess pressures, the maximum at d=0 vanishes.
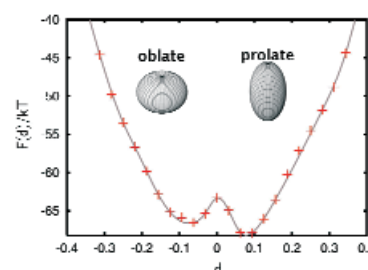

Fig. 2: Free energy F(d) of the asphericity d.

Vesicles Adhering to a Substrate

In living organisms as well as in biomimetic systems, cells or vesicles are often adhering to a substrate. Prominent examples are biosensors in which cells are in contact with metallic electrodes [5]. An important quantity is the adhesion strength W, i.e. the adhesion energy per adhering membrane area. It depends on the material properties of the membrane and the substrate and is often difficult to measure in the experiment.

With Monte Carlo simulations we studied systematically the adhesion behavior of a vesicle with a total area A and bending rigidity κ as a function of the temperature T, the adhesion strength W, and the range s of the adhesion potential (see **Fig. 3**).
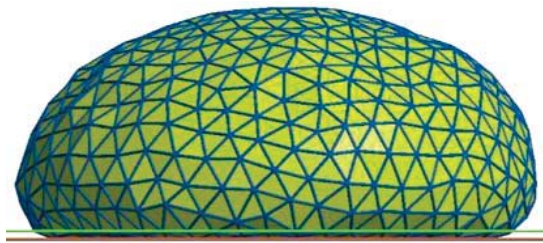

Fig. 3: Snapshot of an adhering vesicle.

We considered vesicles in the absence of osmotically active molecules [6] as well as vesicles with osmotically stabilized volumes V. In both cases it is found that the relative adhesion area A_{ad}/A is a linear function of T/κ if the temperature is not too large. An example is given in **Fig. 4**. With and without osmotically active molecules the dependence of A_{ad}/A on the parameters W, κ, T, s, and, eventually, V can be expressed in a simple formula. If s is approximately known and κ is not strongly temperature-dependent, the formulas can be used to determine W and κ by measuring the adhesion area for two different temperatures.
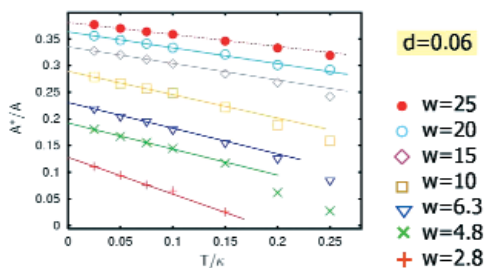

Fig. 4: Relative adhesion area A_{ad}/A as a function of T/k for various values of $w=WA/(2\pi\kappa)$.

Vesicle Transport through Small Pores

A pharmacological application of vesicles is the transport of medically active substances. One important aspect is the transport of vesicles through skin pores which allows carrying active agents into deeper skin regions. It is predicted that the vesicles are pushed through a skin pore by a transdermal concentration gradient of osmotically active molecules. With the help of computer simulations we have found that different molecular concentrations c_1 and c_2 on each side of a small pore is indeed able to drag a vesicle through it **(Fig. 5)**. In the simulations we calculate the free energy barrier $F(A_2)$ for the partial area A_2 having passed the pore. As shown in **Fig. 6** the barrier vanishes for a sufficiently large concentration c_1 and the vesicle is pushed through the pore. The time needed to pass the pore was estimated to be about 70 seconds.
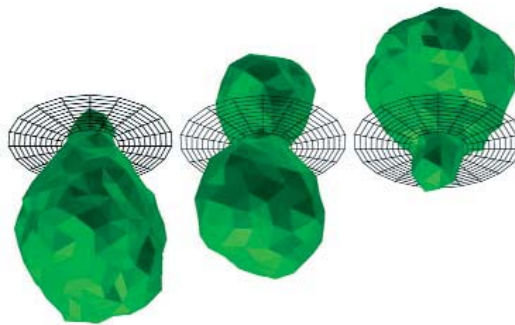
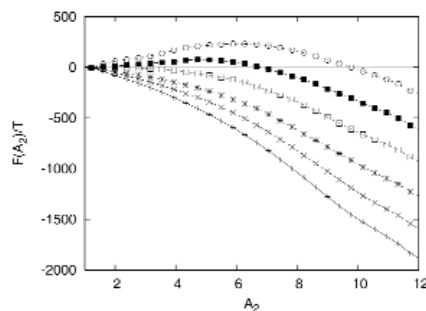

Fig. 5: Snapshots of a vesicle moving though a pore.

Fig. 6: Free energy barrier for a vesicle moving through a pore.

T. Gruhn, E. Gutlederer, G. Linke, R. Lipowsky
Thomas.Gruhn@mpikg.mpg.de

References:

[1] Lipowsky, R.: Generic Interactions of Flexible Membranes. Handbook of Biological Physics Vol. 1, edited by R. Lipowsky, E. Sackmann (Elsevier, Amsterdam, 1995).

[2] Veatch, S.L. and Keller, S.L.: Separation of Liquid Phases in Giant Vesicles of Ternary Mixtures of Phospholipids and Cholesterol. Biophysical Journal **85**, 3074-3083 (2003).

[3] Cevc, G.: Lipid Vesicles and other Colloids as Drug Carriers on the Skin. Advanced Drug Delivery Reviews **56**, 675-711 (2004).

[4] Linke, G., Lipowsky, R., Gruhn, T.: Free Fluid Vesicles are not Exactly Spherical. Physical Review E, accepted.

[5] Arndt, S. et al.: Bioelectric impedance assay to monitor changes in cell shape during apoptosis. Biosensors & Bioelectronics **19**, 583-594 (2004).

[6] Gruhn, T., Lipowsky, R.: Temperature Dependence of Vesicle Adhesion. Phys. Rev. E *71*, 011903-011912 (2005).

INTERDEPARTMENTAL ACTIVITIES

Ions Interacting with Membranes and Polymers and in-between Comes Water

Rumiana Dimova 06.04.1971
1995: Diploma, Chemistry (Sofia University, Bulgaria), Major: Chemical Physics and Theoretical Chemistry, Thesis: Role of the Ionic-Correlation and the Hydration Surface Forces in the Stability of Thin Liquid Films
1997: Second MSc (Sofia University, Bulgaria) Thesis: Interactions between Model Membranes and Micron-Sized Particles
1999: PhD, Physical Chemistry (Bordeaux University, France) Thesis: Hydrodynamical Properties of Model Membranes Studied by Means of Optical Trapping Manipulation of Micron-Sized Particles
2000: Postdoc (Max Planck Institute of Colloids and Interfaces, Potsdam)
Since 2001: Group Leader (Max Planck Institute of Colloids and Interfaces, Potsdam)

References:
[1] Sinn, C., Antonietti, M. and Dimova, R.: Binding of calcium to phosphotidyl-phosphoserine membranes. in preparation.
[2] Franke, T.: Haftübergang von Lipid-Vesikeln: Effekt von CrCl₃ auf PC-Membranen. PhD Thesis (2003).
[3] Haluska, C.: Interactions of functionalized vesicles in the presence of europium (III) chloride. PhD Thesis (2005).
[4] Sinn, C., Dimova, R. and Antonietti, M.: Isothermal titration calorimetry of the polyelectrolyte/water interaction and binding of Ca^{2+}: Effects determining the quality of polymeric scale inhibitors. Macromolecules, **37**, 3444-3450 (2004).
[5] Dimova, R., Lipowsky, R., Mastai Y. and Antonietti, M.: Binding of polymers to calcite crystals in water: Characterization by isothermal titration calorimetry. Langmuir **19**, 6097-6103 (2003).

Ion-membrane interactions are important for the physiological activity of cells as they are inherent to almost every cellular process. Synthetic polymers on the other hand are artificial analogs to macromolecules like proteins and nucleic acids whose conformation and properties also strongly depend on the presence of ions. One example of ion-protein interactions is the renowned but still poorly understood Hofmeister series, which arranges different ions according to their ability to induce precipitation of egg white proteins. Overall, the behavior of both, membranes and polymers (artificial or natural), is influenced by interactions with ions. Intuitively, one would expect that electrostatic forces have the most prominent contribution to these interactions. However, the experiments we have performed in the last few years show that the polar character of a trivial molecule like water plays an even more important role. We have found that changes in water structure, i.e., destroying and reforming hydration shells, breaking hydrogen bonds, appears to be the driving force in many ion-membrane and ion-polymer interactions.

A convenient technique for studying these processes is isothermal titration calorimetry (ITC). ITC can be used to measure ion-membrane and ion-polymer interaction enthalpy. When an appropriate model is applied, the titration calorimetry data can be used to extract the equilibrium constant of the process, i.e., characterize the stoichiometry of the interaction. Calcium, chromium and lanthanide ions (like europium and gadolinium) are among the ions that have been studied in our lab **[1-3]**. They were used to probe the properties and stability of large unilamellar vesicles (~100nm in size). All of the ions yield endothermic signals when titrated into the vesicle solution. Even when the lipid membrane is negatively charged, calcium was found to interact with an endothermic signal ($\Delta H > 0$) **[1]**.

The results obtained were consistent with measurements investigating ion-polymer interactions. We studied adsorption of calcium to polymers having the same functional groups as those of the charged membranes **[4]**. Once again, the driving factor of the process was found to be the entropy gain from liberating water molecules (see **Fig. 1B**).
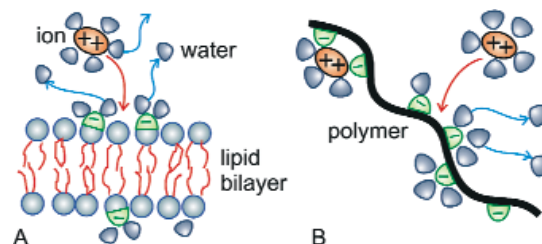

Fig. 1: Schematic presentation of the interaction of a multivalent cation with a negatively charged lipid bilayer (A) and with a polymer (B). The ion size is exaggerated for clarity. The process is driven by the liberation of water molecules from the hydration shells of the ions and the membrane/polymer charges.

The interaction of calcium with polymers was also studied in the context of crystal growth and scale inhibition. In a similar fashion, binding of polymers to calcite crystals was found to be endothermic and entropy driven **[5]**. This indicates that structure of water plays an important, currently not fully recognized role in the control of mineralization processes.

We have found that the ion-membrane and ion-polymer interaction is endothermic ($\Delta H > 0$). For the measured processes to occur spontaneously, the condition $T\Delta S > 0$ (where T is temperature and ΔS is entropy change) has to apply which implies that the interactions are entropically driven. The gain in entropy is presumably due to destruction and reassembly of hydrations shells finally resulting in the liberation of water molecules, see **Fig. 1**. All of our results point to the importance of the restructuring of water as a driving force in ion-membrane and ion-polymer interactions.

In addition to the thermodynamic characterization we are able to observe the ion-membrane interaction directly using microscopy. Our measurements on giant unilamellar vesicles (~10μm in radius) show that multivalent ions induce adhesion between two neutral membranes **[2, 3]**. In addition, small amount of europium or calcium ions were found to cause membrane rupture presumably due to ion-generated membrane tension. The current working hypothesis is that the ions have condensing effect on lipid molecules, i.e. they reduce the area per lipid, thus bringing about membrane tension and causing eventual rupture.

R. Dimova, M. Antonietti, T. Franke, C. Haluska, R. Lipowsky, Y. Mastai, C. Sinn
Rumiana.Dimova@mpikg.mpg.de

MEMBRANES AND VESICLES

Effect of Electric Fields on Model Membranes; "Squaring" the Vesicle

The interaction of electric fields with lipid membranes and cells has been extensively studied in the last decades. The phenomenon of electroporation is of particular interest because of its vast use in cell biology and biotechnology. Strong electric pulses of short duration induce electric breakdown of the lipid bilayer. The membrane becomes permeable for a certain time because of transient pores across the bilayer allowing the influx/efflux of molecules. Thus, electroporation is often used to introduce molecules like proteins, foreign genes (plasmids), antibodies, or drugs into cells. Even though a lot is known about the phenomenology of cell electroporation, the mechanism of pore opening across the lipid matrix is still not fully understood. Experiments on giant vesicles are of special relevance because their size is comparable to cells and allows for direct observation using optical microscopy. In the presence of electric fields, lipid vesicles are deformed because of the electric stress imposed on the lipid bilayer given by the Maxwell stress tensor. This effect has been studied theoretically both for alternating fields and for square-wave pulses [1] but few experiments have been performed so far.

The application of AC fields induces shape transformations on giant vesicles. The experiments in our lab (PhD project of Said Aranda) show that phospholipid vesicles subject to AC fields undergo prolate or oblate shape deformation depending on two factors: the frequency of the applied field, ω, and the conductivity ratio between the solution inside and outside the vesicle, σ_{in}/σ_{out}. Based on our results we have constructed a phase diagram that describes the vesicle morphology in response to ω and σ_{in}/σ_{out}.

Microscopy observation of effects caused by electric DC pulses on giant vesicles is difficult because of the short duration of the pulse. Recently this difficulty has been overcome in our lab. Using a digital camera with high temporal resolution we were able to access vesicle dynamics on a sub-millisecond time scale (1 image every 33 µs) [2]. The shape deformation induced on lipid vesicles by square-wave pulses was found to depend strongly on σ_{in}/σ_{out}. In the absence of salt spherical vesicles assume a prolate shape as a response to the external field, with the long symmetry axis aligning parallel to field direction, see **Fig. 1**.

For strong enough pulses, electroporation was observed generally accompanied by formation of visible macropores in the micrometer size range **(Fig. 1)**. The response of the system (change in the vesicle aspect ratio, pore lifetime and pore radius) was interpreted in terms of membrane properties like stretching and bending elasticity, surface viscosity, edge energy, and the media viscosity [2].

In addition, the conductivity ratio was demonstrated to play an important role on the vesicle deformation. Depending on σ_{in}/σ_{out} the vesicle can assume prolate or oblate shapes, similar to results obtained in experiments on vesicles in AC fields. Moreover, the DC pulses induce cylindrical deformation as observed for the first time in our lab [3], see **Fig. 2**. Surprising barrel-like shapes were seen only in the case when salt was present in the vesicle exterior.
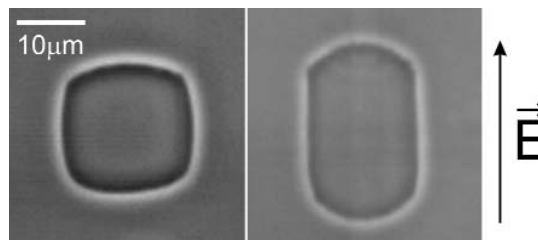
Fig. 2: "Squared" vesicles. In presence of salt in the vesicle exterior high voltage pulses induce short-lived "squared" shapes (due to axial symmetry around the field direction the vesicles should actually be cylindrical).

R. Dimova, S. Aranda, K. A. Riske
Rumiana.Dimova@mpikg.mpg.de

References:
[1] Kummrow, M. and Helfrich, W.: Deformation of giant lipid vesicles by electric fields. Phys. Rev. A. **44**, 8356-8360 (1991); Hyuga, H., Kinosita, K. Jr., and Wakabayashi, N.: Deformation of vesicles under the influence of strong electric fields. Jpn. J. Appl. Phys. **30**, 1141-1148 (1991); ibid. Jpn. J. Appl. Phys. **30**, 1333-1335 (1991).
[2] Riske, K.A., and Dimova, R.: Electro-deformation and -poration of giant vesicles viewed with high temporal resolution. Biophys. J. **88**, 1143-1155 (2005).
[3] Riske, K. A., Lipowsky, R. and Dimova, R.: High temporal resolution of electro-poration, fusion and deformation of giant vesicles. "Squaring" the vesicles. Biophys. J. **86**, 518a (2004).
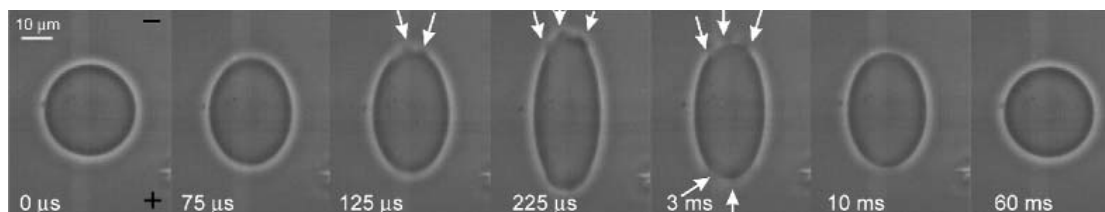

Fig. 1: A snapshot sequence of a vesicle subjected to a pulse of strength 2 kV/cm and duration 200 µs. The vesicle assumes prolate shape elongated along the field direction (the electrode's polarity is indicated with a plus and a minus sign on the first snapshot). Macropores are first visualized in the third frame (125 µs).

MEMBRANES AND VESICLES

Thermal Fluctuations and Elasticity of Lipid Membranes

Wilhelm Fenzl 15.9.1949

1978: Diploma, Physics (Ludwig-Maximilians-Universität München) Thesis: Röntgenographische Untersuchung von Wasserstoff in Palladium-Silber-Legierungen

1983: PhD, Physics (Ludwig-Maximilians-Universität München) Thesis:Phasenübergänge und Korrelation von Wasserstoff in Niob-Molybdän Legierungen

1983-1990: Research Assistant (Ludwig-Maximilians Universität München)

1990: Habilitation, Physics (Ludwig-Maximilians-Universität München) Thesis: Fluide Grenzflächen

1991-1994: Research Scientist (Institut für Festkörperforschung, Forschungszentrum Jülich)

Important model systems for biological membranes are phospholipid bilayers, which are intensively studied with regard to structure, phase transitions, transport and elasticity properties, as well as interaction with other macromolecules. From the point of view of statistical mechanics they represent an interesting class of fluctuating quasi two-dimensional objects whose thermal fluctuations are governed by the intrinsic bending rigidity κ. The effect of the thermal fluctuations on the positional correlations and the scattering intensity distribution has been worked out in the framework of linear elasticity theory (Caillé model) for stacks with periodic boundary conditions, as a function of κ and the compressional modulus B (given by the second derivative of the interaction potential between two membranes at their equilibrium distance d). Recently, the model has been extended to include the boundary condition of a flat substrate on which a stack of lipids can be deposited [1-4].

X-ray experiments to study thermal fluctuations of lipid membranes have been carried out on samples with several hundreds of highly oriented membranes deposited on silicon surfaces and studied at full hydration under excess water [5]. The main aim was to map the diffuse scattering over a wide range of momentum transfer, see **Fig. 1** (a), both in radial q_r (parallel to the plane of the membrane) and q_z. Diffuse x-ray reflectivity measurements using 20 keV synchrotron beams have been carried out at the undulator beamline ID1 (ESRF), using both a fast scintillation counter and a multiwire area detector. Data was collected on the uncharged lipids DMPC and POPC. For data acquisition the angles of incidence were chosen so that specular Bragg peaks are not excited. The typical intensity distribution on the CCD detector then consists of only a weak specular beam and two to four strong equidistant diffuse Bragg sheets. From the q_z value, the mean distance d can be obtained, i.e. for fully hydrated DMPC membranes $d \approx 63$ Å, corresponding to a water layer of about *25 Å* in between adjacent membranes. Importantly, the width (HWHM) of the diffuse Bragg sheets along q_z increases quadratically with q_r, before it saturates at high q_r, see **Fig. 1** (c) for a typical data set. The quadratic increase (solid line) is in line with the theoretic prediction and its steepness is given by the fundamental smectic length $\lambda = (\kappa /Bd)^{0.5}$. From the analysis of the q_z-integrated intensity the height–height correlation function can be determined using a back transformation method. The resulting curve for DMPC in the fluid phase is shown in **Fig. 1**(c) along with theoretic curves (solid lines) [4]. The parameters κ and B can be chosen to fit the curves at small, intermediate or large r, but should be regarded as effective parameters, which can vary significantly since the model cannot account for all data simultaneously.

Already on the level of the raw data, deviations from the predicted behavior are observed: (i) for the power law exponent of the intensity decay shown in **Fig. 1** (d), and (ii) for the saturation of the Bragg sheet width shown in **Fig. 1** (b). Both are observed at parallel wave vector components which were not accessible before (in randomly oriented bilayers or at less brilliant sources). Therefore we must conclude that fluctuations on the corresponding length scales are not well described by the Caillé model. A number of reasons could limit the applicability of the model: (i) non-bending collective motions, (ii) non-linear elasticity terms, (iii) a length scale dependence of *K*, (iv) breakdown of the mean field approach. Alternative more rigorous theories (renormalization group theories, self-consistent theories) and computer simulations on reasonably large stacks of membranes and lateral system size may help to gain more understanding.

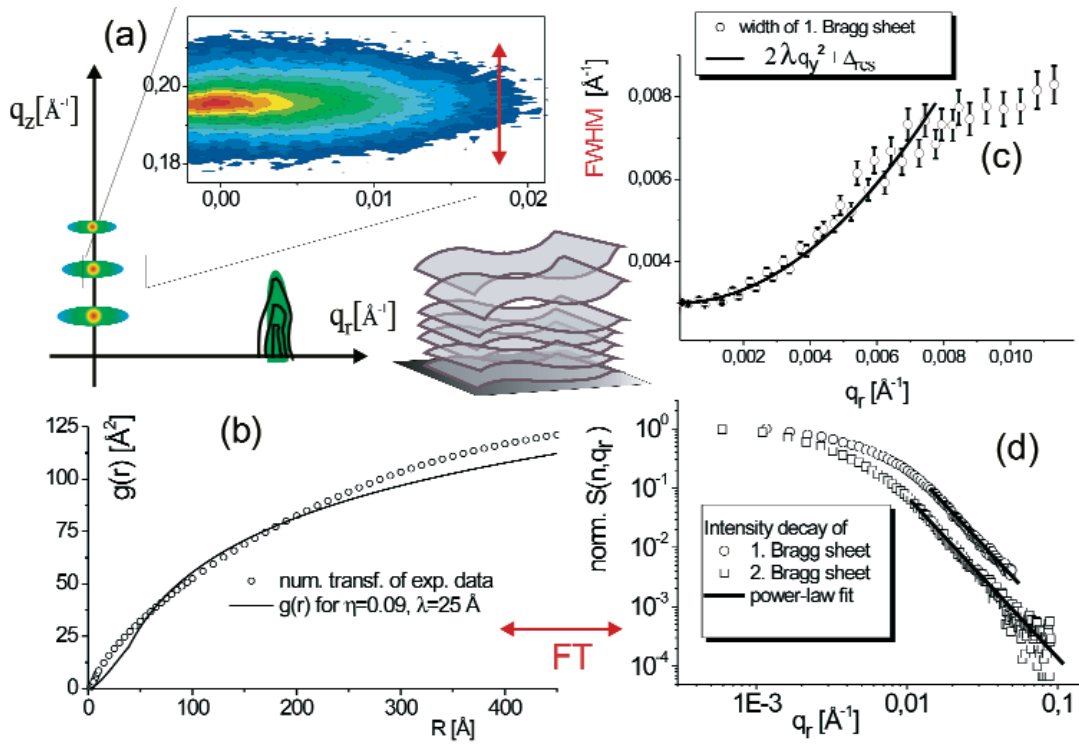W. Fenzl

wilhelm.fenzl@physik.uni-muenchen.de

References:

[1] Vogel, M., Münster, C., Fenzl, W. and Salditt, T.: Thermal Unbinding of Highly Oriented Phospholipid Membranes, Phys. Rev. Lett. **84**, 390 (2000).

[2] Vogel, M.: Röntgenbeugung an hochorientierten Phospholipid-membranen, Dissertation, Univ. Potsdam (2000).

[3] Vogel, M., Münster, C., Fenzl, W., Thiaudiere, D., Salditt, T.: Fully hydrated and highly oriented membranes: an experimental setup amenable to specular and diffuse X-ray scattering, Physica B **283**, 32-36 (2000).

[4] Constantin, D., Mennicke, U., Li, C. and Salditt, T.: Solid-supported multilayers: Structure factor and fluctuations, Eur. Phys. J. E **12**, 283 (2003).

[5] Salditt, T., Vogel, M., Fenzl, W.: Thermal Fluctuations and Positional Correlations in Oriented Lipid Membranes, Phys. Rev. Lett. **90**, 178101 (2003).

Fig. 1: (a) Typical diffuse scattering distribution of multilamellar lipid bilayers (DMPC, fluid phase) (b) Characteristic height-height self-correlation function of an averaged membrane in the stack as derived from the data, together with theoretic function acc. to [4]. (c) Increase in the width (vertical q_z-width) of the first Bragg sheet. (d) Decay of the (q_z-) integrated intensity of the the first two Bragg sheets n=1 and n=2.

Membrane Adhesion

Thomas Weikl 01.04.1970
1996: Diploma, Physics
(Freie Universität Berlin)
Thesis: Interactions of rigid
membrane inclusions
1999: PhD, Physics
(Max Planck Institute of Colloids
and Interfaces, Potsdam)
Thesis: Adhesion of
multicomponent membranes
2000-2002: Postdoc
(University of California,
San Francisco)
Since 2002: Group Leader
(Max Planck Institute of Colloids
and Interfaces, Potsdam)

In the classic fluid-mosaic model of Singer and Nicolson, biological membranes are envisioned as lipid bilayers with embedded or adsorbed proteins. Recent research on membranes emphasizes two important 'updates' of this picture: First, biological membranes contain *domains* of different composition, and second, *active processes* play a central role for many membrane functions. Our theoretical models of membranes and membrane adhesion are focused on these two novel aspects.

In principle, the formation of membrane domains can be driven by a demixing of the lipid bilayer, or by the aggregation of membrane proteins. Our research here focuses on protein aggregation, in particular during membrane adhesion. The adhesion of biological membranes is mediated by various types of receptors and ligands, also called 'stickers'. These stickers often differ in their characteristic binding lengths. The length difference leads to an indirect, membrane-mediated repulsion between long and short stickers, simply because the lipid membranes have to be curved to compensate the length mismatch, which costs bending energy. The membrane-mediated repulsion causes a lateral phase separation into domains containing short and domains containing long stickers (see **Fig. 1**). In general, the lateral phase behavior depends on the sticker concentrations. Lateral phase separation can only occur if the sticker concentrations exceed a critical threshold. An additional driving force for phase separation comes from large, repulsive glycoproteins, which form a steric barrier for the binding of short stickers. The rich equilibrium phase behavior of such membranes can be characterized using scaling estimates and Monte Carlo simulations.
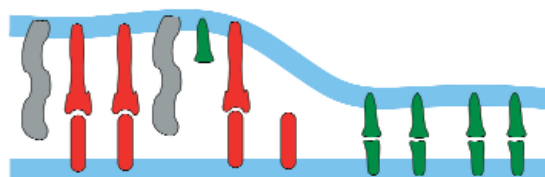

Fig. 1: Domain formation in membranes adhering via short (green) and long (red) receptor-ligand complexes, or 'stickers'. The domains are caused by the length mismatch between the complexes. Repulsive glycoproteins (grey) pose a steric barrier for the short sticker complexes and constitute an additional driving force for the domain formation.

The protein domains in biological membranes are often highly dynamic. Intriguing examples are the domain patterns formed during T cell adhesion. The patterns are composed of domains which either contain short TCR/MHCp receptor-ligand complexes or the longer LFA-1/ICAM-1 complexes. The domain formation is driven by the length difference between the TCR/MHCp and the LFA-1/ICAM-1 complexes. During T cell adhesion, the domains evolve in a characteristic pattern inversion: The final pattern consists of a central TCR/MHCp domain surrounded by a ring-shaped LFA-1/ICAM-1 domain, whereas the characteristic pattern formed at intermediate times is inverted with TCR/MHCp complexes at the periphery of the contact zone and LFA-1/ICAM-1 complexes in the center.

We have studied the pattern formation dynamics in a statistical-mechanical model for the adhesion of multicomponent membranes [1,3]. In this model, the adhesion geometry of the cells is taken into account by dividing the membranes into a contact zone and a non-adhering membrane region (see **Fig. 2**).
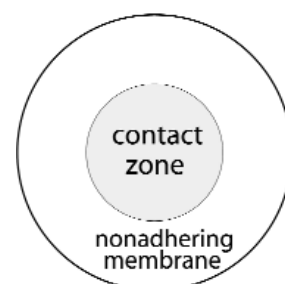

Fig. 2: Cell adhesion geometry. The circular contact zone is surrounded by a nonadhering membrane ring. Receptors, ligands, and glycoproteins diffuse around in the whole membrane, but interact with the apposing membrane only within the contact zone.

We consider the pattern formation in Monte Carlo simulations (see **Fig. 3**) and propose a novel self-assembly mechanism for the formation of the intermediate inverted T-cell pattern. This mechanism is based (i) on the initial nucleation of numerous TCR/MHCp microdomains, and (ii) on the diffusion of free receptors and ligands into the cell contact zone. The diffusion of receptors and ligands into the contact zone leads to the faster growth of peripheral TCR/MHCp microdomains and to a closed ring for sufficiently large TCR/MHCp concentrations. At smaller TCR/MHCp concentrations, we observe a second regime of pattern formation with characteristic multifocal intermediates, which resemble patterns observed during adhesion of immature T cells or thymozytes. The formation of the final T-cell pattern requires active cytoskeletal transport processes in our model, in agreement with experimental findings [3].

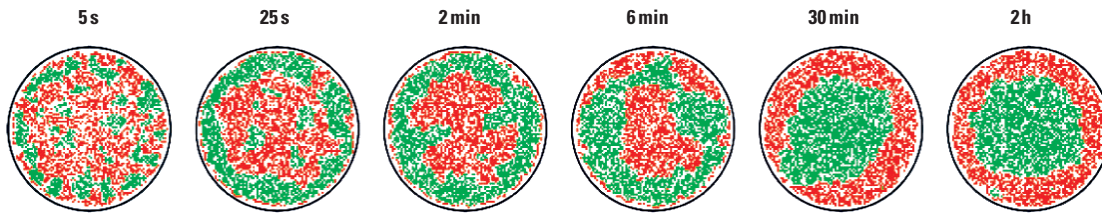| 5 s | 25 s | 2 min | 6 min | 30 min | 2 h |

Fig. 3: Simulated pattern formation during T cell adhesion. Within the first minute of adhesion, a peripheral ring of short TCR/MHCp complexes (green) is formed, surrounding a central domain of long ICAM-1/LFA-1 complexes (red). After 30 minutes, this pattern is inverted and a central TCR/MHCp domain emerges.

Active processes also play a role in controlling the adhesiveness of biological membranes. We have considered a simple theoretical model of membranes with active adhesion molecules, or 'stickers' [4]. The stickers are actively switched 'on' or 'off', which keeps the system out of thermal equilibrium. We find that the phase behavior of the membranes depends rather sensitively on the switching rates of the stickers and not only on the fraction of 'on'-stickers. In asymptotic regimes of 'slow' and 'fast' switching, we obtain exact results that relate the unbinding behavior of the active membranes to well-studied properties of equilibrium membranes. At intermediate switching rates, we observe resonance and weak binding in Monte Carlo simulations. These results may provide insights into novel mechanisms for the controlled adhesion of biological or biomimetic membranes.

Membranes elastically mediate interactions also between curved objects adhering to them [2]. These membrane-mediated interactions are related to those between long and short stickers. The adhesion of curved objects such as rods or beads causes a local perturbation of the equilibrium membrane shape, which leads to the indirect, membrane-mediated interactions. For a planar membrane under a lateral tension, the interaction between two parallel rods is repulsive if the rods adhere to the same side of the membrane, and attractive if the rods adhere at opposite membrane sides. For a membrane in an external potential, the membrane-mediated interactions between adsorbed rods are always attractive and increase if forces perpendicular to the membrane act on the rods.

T. R. Weikl, M. Asfaw, R. Lipowsky, B. Rozycki
thomas.weikl@mpikg.mpg.de

References:
[1] Weikl, T.R., Groves, J.T. and Lipowsky, R.: Pattern formation during adhesion of multicomponent membranes. Europhys. Lett. **59**, 916-922 (2002).
[2] Weikl, T.R.: Indirect interactions of membrane-adsorbed cylinders. Eur. Phys. J. E **12**, 265-273 (2003).
[3] Weikl, T.R. and Lipowsky, R.: Pattern formation during T cell adhesion. Biophys. J. **87**, 3665-3678 (2004).
[4] Rozycki, B., Lipowsky, R. and Weikl, T.R.: Adhesion control of membranes via active stickers. in preparation.

Mastering Membrane Fusion

Rumiana Dimova 06.04.1971
1995: Diploma, Chemistry (Sofia
University, Bulgaria), Major: Chemical
Physics and Theoretical Chemistry,
Thesis: Role of the Ionic-Correlation
and the Hydration Surface Forces in
the Stability of Thin Liquid Films
1997: Second MSc
(Sofia University, Bulgaria)
Thesis: Interactions between Model
Membranes and Micron-Sized Particles
1999: PhD, Physical Chemistry
(Bordeaux University, France)
Thesis: Hydrodynamical Properties
of Model Membranes Studied by
Means of Optical Trapping
Manipulation of Micron-Sized Particles
2000: Postdoc (Max Planck Institute
of Colloids and Interfaces, Potsdam)
Since 2001: Group Leader
(Max Planck Institute of Colloids
and Interfaces, Potsdam)

Membrane fusion is an exciting but relatively complex phenomenon. In real cells it involves the participation of a number of so called fusogenic proteins who are thought to perform the role of a recognition system that brings two membranes together, perturbs the lipid bilayers, and eventually assists the lipid mixing. The fusion process is of significant importance as it is involved in vital cellular functions like import of food stuff and export of waste (endo- and exocytosis), fertilization, signaling in nerve cells and others. Experimental tools for the controlled fusion of membranes should be essential in order to improve and optimize fusion applications like drug delivery, artificial fertilization and gene transfer.

Thus, achieving control on fusion has been the driving force for initiating experiments on model membranes. The most popular bilayer system on which fusion was studied are solutions of small unilamellar vesicles (LUVs) of ~100nm in size. However, in such systems the fusion efficiency is set rather indirectly, the measured properties are determined by the bulk solution (and not by individual vesicle pairs) and thus represent averages over a large number of vesicles. In addition, due to the small size, the behavior of LUVs may be governed by membrane tension and high curvature effects. In contrast, applying optical microscopy to follow interactions between giant unilamellar vesicles (GUVs) gives access to direct observation of fusion events. The GUV size (~10µm) brings the model systems up to the level where the membrane dimensions are of cell-size. In the last decade, several powerful tools such as micropipette aspiration have been developed to allow the experimental manipulation of GUVs. Combining optical microscopy with micropipettes is a rather promising route for studying and achieving control over membrane fusion.

Recently, the investigation of two types of fusion-inducing mechanisms in GUVs was initiated in our lab. In one of them, the inter-membrane interaction is triggered by metal ions forming complexes between functionalized molecules in the bilayers. In the second approach, we apply strong electric pulses to vesicles in contact. In both cases fusion is induced. Using high speed digital imaging we follow the evolution of the fused membranes with unprecedented time resolution of about 50µs. Fusion dynamics as reported in the literature has been limited, so far, to time resolution of about 1ms. For the first time, we were able to observe the opening of the fusion pore with high temporal resolution.

Fusion of Functionalized Membranes:

The membranes are functionalized with synthetic fusogenic molecules [1] which can form a complex with multivalent ions. The fusogenic molecules have a lipid-like structure with hydrophilic headgroup containing a specific ligand. The ligands form coordination complexes with metal ions in 2:1 ratio. When the complexes are formed between ligands from opposing membranes, the expected event is fusion. This fusion scenario was probed in our lab [2] by means of manipulating two vesicles with micropipettes. A third micropipette was used to locally inject a solution of multivalent ions. The ions were observed to induce adhesion between the two vesicles, which was followed by fusion. **Fig. 1** is a simplified cartoon of the possible fusion mechanism occurring at molecular level. The resolution of optical microscopy (~0.5µm) limits the observation to the micrometer scale and the molecular events cannot be revealed. Thus it is not clear how many complexes are involved in the fusion event.
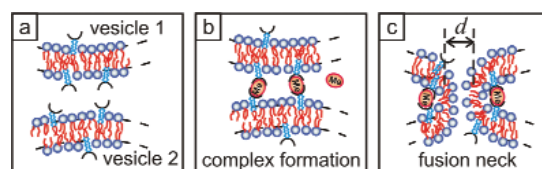

Fig. 1: Possible steps in the fusion of functionalized membranes: (a) two functionalized lipid vesicles are brought into contact; (b) a solution of multivalent ions is locally injected in the contact area leading to the formation of inter-membrane complexes; (c) the opening of the fusion neck is initiated.

Electrofusion:

When exposed to weak AC field, vesicles align in the direction of the field. This can bring two vesicles into contact. The subsequent application of DC pulses leads to charging of the membrane. This creates transmembrane potentials which are enhanced at the vesicle poles (facing the electrodes). The corresponding compression of the membrane effectively induces tension. DC pulses can lead to perforation of the membrane in two cases [3]: (i) when the transmembrane potential exceeds some critical value (~1V); or (ii) when the total membrane tension approaches the lysis tension of the membrane (~5dyn/cm). When poration is induced in the contact area of two vesicles, fusion is expected to occur. **Fig. 2** illustrates a possible mechanism of electrofusion of two bilayers in contact.
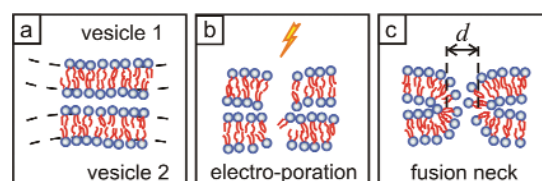

Fig. 2: Possible steps in electrofusion: (a) two lipid vesicles are brought into contact and aligned using AC field; (b) a short electric pulse is applied causing membrane poration; (c) the lipids from the opposing bilayers mix initiating the opening of the fusion neck.

In the experiments, the vesicles are placed between two electrodes and then observed with phase contrast microscopy. One example of a fusion event observed with a fast digital camera and phase contrast microscopy is presented in **Fig. 3**. The two vesicles were aligned by an AC field applied prior to the DC pulse. Time t=0 corresponds to the beginning of the pulse. A closer look at the micrograph sequence (not all of the acquired snapshots are displayed) shows that fusion has already occurred within the first 50µs. Using intensity profile image analysis, we are able to follow the evolution of the opening of the fusion neck diameter, d, (see F**ig. 1c** and **Fig. 2c**). The experiments extend over five orders of magnitude in time, ranging from microseconds to seconds. Two characteristic times are revealed, presumably corresponding to two different processes: molecular rearrangement of the lipid bilayers related with relaxation of the edge curvature of the fusion pore (t~1ms), and hydrodynamics of mixing of the fluid contents of the fusing vesicles.

In certain cases, when electrofusion is induced, multiple fusion events are observed (the example in **Fig. 3** illustrates one of them). The reason for this behavior is that the fusing vesicles have porated at several places. This leads to reclosure of the membrane inside the product vesicle and to formation of smaller internalized vesicles (one can see this in **Fig. 3** at t=10s where the internal vesicles appear as brighter spots inside the resulting vesicle; the brighter gray values are due to refractive index mismatch of the vesicle contents).

In conclusion, we have achieved controlled fusion induced by two approaches: ligand mediated fusion and electrofusion. The tools available in our lab have allowed us to reach unprecedented time resolution of the fusion process.

R. Dimova, C. Haluska, R. Lipowsky, K. A. Riske,
Rumiana.Dimova@mpikg.mpg.de

References:
[1] Richard, A., Marchi-Artzner, V., Lalloz, M.-N., Brienne, M.-J., Artzner, F., Gulik, T., Guedeau-Boudeville, M.-A., Lehn, J.-M.: Fusogenic supramolecular systems of vesicles induced by metal ion binding to amphiphilic ligands. Proc. Nat. Acad. Sc. **101**, 15279-15284 (2004).
[2] Haluska, C.: Interactions of functionalized vesicles in the presence of europium (III) chloride. PhD Thesis (2005).
[3] Riske, K.A., and Dimova, R. : Electro-deformation and -poration of giant vesicles viewed with high temporal resolution. Biophys. J. **88**, 1143-1155 (2005).
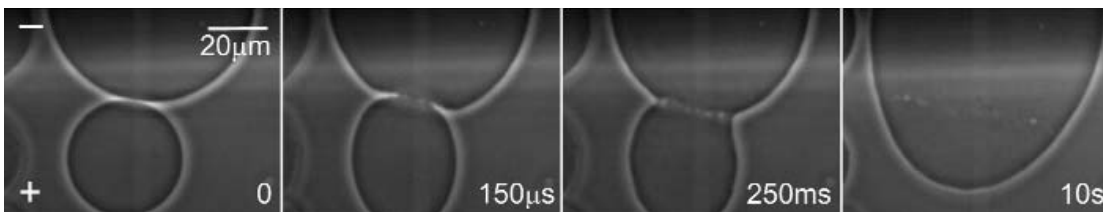
Fig. 3: Snapshot sequences of electrofusion of a vesicle couple. The time is indicated on each snapshot. The electrodes polarity is indicated with a plus (+) and a minus (-) sign on the first snapshots. The image acquisition rate was 30,000fps. The applied pulse has a strength of 90V and a duration of 150µs.

Free and Tethered Polyelectrolytes

Polyelectrolytes (PELs) are macromolecules that contain subunits having the ability to dissociate charges in polar solvents such as, e.g., water. Due to their importance in materials science, soft matter research, and molecular biology, PELs have received a lot of attention in recent years.

With respect to different dissociation behaviors, one can distinguish between strong and weak PELs, a classification used among chemists, or between quenched and annealed PELs, the common classification in the physics community. Strong PELs, poly-salts such as, e.g., Na-PSS, dissociate completely in the total pH range accessible to experiment. The total charge as well as its particular distribution along the chain is solely imposed by polymer synthesis. On the other hand, weak PELs represented by poly-acids and poly-bases dissociate in a limited pH range only. The total charge of the chain is not fixed but can be tuned by changing the solution pH. The number of charges as well as their distribution is a fluctuating thermodynamic variable. The control parameter is the solution pH which is, up to trivial additive constants, the chemical potential of the charges μ.

Polymer brushes consist of chains densely end-grafted to a surface. Due to various forces, tethered chains are enforced to take an elongated conformation. PEL brushes form the subject of increasing interest in theory, simulation and experiment. From the application point of view, they are an effective means for, e.g., preventing colloids from flocculation. PEL brushes can be used in small devices for pH-controlled gating and are thought to be a model for the protecting envelope of cells (glycocalix).

Annealed Polyelectrolytes in Poor Solvents

We study annealed PELs by semi-grand canonical Monte Carlo simulations where the chains are in contact with a reservoir of charges of fixed chemical potential μ. For sufficiently poor solvent quality, it was recently confirmed [1] that the chains undergo a first-order phase transition between a weakly charged globule and a strongly charged stretched conformation as predicted by theory. However in the close-to-Θ-point regime $\tau < \tau^*$ ($\tau = (\Theta - T)/\Theta$) the conformational transition becomes almost continuous. Changing the degree of ionization by tuning the chemical potential, i.e., by tuning the solution pH, we obtain for the first time a sequence of pearl-necklace transitions in annealed PELs (see **Fig. 1 [2]**). Most of the pearl-necklace parameters are found to obey the scaling relations predicted for quenched PELs. Although there occurs a sequence of discrete transitions embedded in the continuous crossover from globule to stretched chain, due to strong fluctuations the pearl-necklace transition as a whole appears to be continuous.
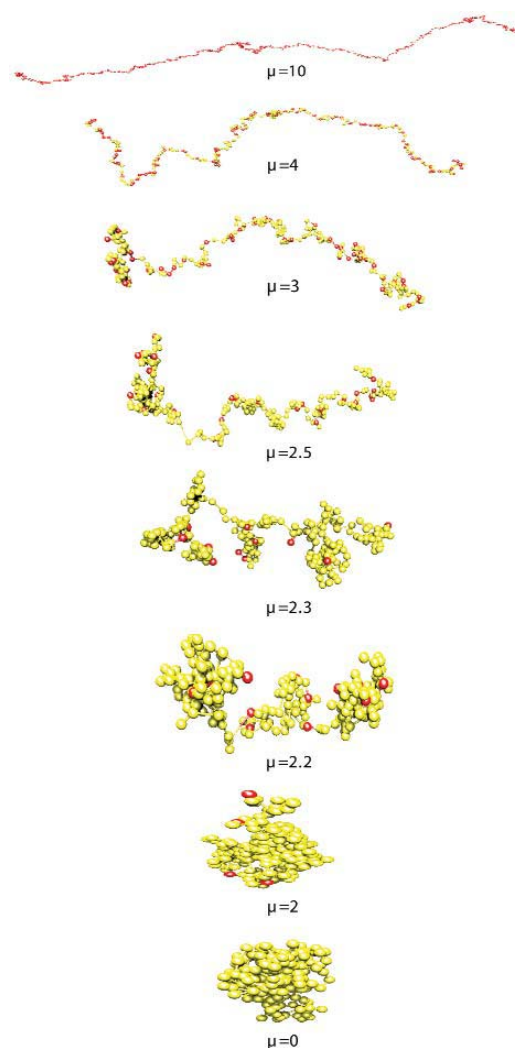
Christian Seidel 07.02.1949

1972: Diploma, Physics
(Technical University Dresden)
Thesis: Calculation of angular
distribution and polarization of nucleon
scattering close to resonance energies

1978: Dr. rer. nat., Polymer Physics
(Institute for Polymer Chemistry,
Teltow) Thesis: On the calculation
of the phonon dispersion of solid
polymers, application to
polyvinylidenfluoride

1979-83: Research Scientist
(Joffe Physico-Technical
Institute, Leningrad)

1983-89: Research Scientist
(Institute for Polymer
Chemistry, Teltow)

1985: Dr. sc. nat.,
Solid State Theory (Institute for
Polymer Chemistry, Teltow)
Thesis: Ground states and critical
temperatures in quasi-one-dimensional
systems

1989-91: Group Leader
(Institute for Polymer Chemistry, Teltow)

Since 1992: Group Leader
(Max Planck Institute of Colloids
and Interfaces, Potsdam)

1994: Habilitation,
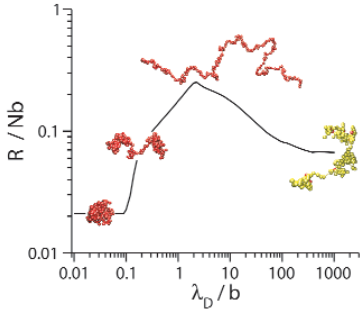Theoretical Chemistry
(Technical University, Berlin)

Fig. 1: Annealed PELs, close-to-Θ-point behavior at $\tau = 0.07$ ($\lambda_B/b = 1$, $\lambda_D/b = 10$). Simulation snapshots taken at varying chemical potential μ: globular structure ($0 \leq \mu \leq 2$), pearl necklaces ($2.2 \leq \mu \leq 2.5$), stretched chain ($3 \leq \mu \leq 10$). Charged monomers are colored red, uncharged yellow.

Varying salt concentration is an important parameter to tune the polyelectrolyte effect and to change the structure of PELs in experiment. Due to the additional charge degree of freedom, annealed PELs exhibit a rather complex behavior. **Fig. 2** shows the end-to-end distance R as a function of the screening length λ_D at moderate chemical potential [3]. At $\lambda_D/b \lesssim 2$ we recover the behavior known from quenched PELs: starting from a globule the chain becomes increasingly stretched with growing λ_D. An interesting feature is visible at $\lambda_D/b \approx 0.1$ where completely charged pearl necklaces exist. Beyond $\lambda_D/b \approx 2$, however, the chain shrinks again. Due to reduced screening the electrostatic penalty of ionization becomes too large and the chain starts to minimize its energy by a partial neutralization of charge. Thus, the polyelectrolyte effect is suppressed although screening is reduced. Clearly the position of maximum stretching depends on the particular chemical potential.

Fig. 2: Annealed PELs, close-to-Θ-point behavior at $\tau = 0.07$ ($\lambda_B/b = 1$, $\mu = 3.0$). Chain extension R vs. screening length λ_D, typical snapshots of the different regimes are shown using the same coloring as in Fig.1.

Polyelectrolyte Brushes

Recently a slight but detectable variation of brush height h on grafting density ρ_a has been obtained both in experimental and simulation studies [4]. This disagrees with the well-accepted scaling relation in the so-called osmotic brush regime, but can be understood on a semi-quantitative level by using a free-volume approximation: The volume available for the counterions $V_0'' = h / \rho_a$ is reduced by the self-volume of the chain $\upsilon = Nb\sigma_{eff}^2$, where σ_{eff} takes into account the monomer and counterion diameters. Thus the free-volume is given by $V'' = V_0'' (1 - \eta)$, with η being the degree of close-packing in the brush. Balancing the resulting nonlinear entropy of counterions with the high-stretching chain elasticity, the equilibrium brush height depends on ρ_a indeed. **Fig. 3** shows simulation results with various theoretical predictions where the nonlinear theory was evaluated with $\sigma_{eff}^2 = 2\sigma^2$ and σ is the Lennard-Jones radius that governs the range of short-range interaction [4].
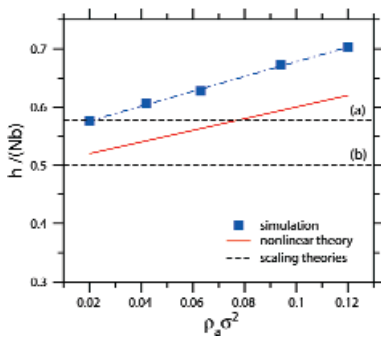

Fig. 3: Brush height as a function of grafting density ρ_a for completely charged polyelectrolyte chains ($\lambda_B/b = 1$). Symbols show simulation data with corresponding linear fit (dot-dashed line); the straight solid line gives the prediction of the nonlinear theory. The dashed lines show previous scaling predictions.

According to Pincus [5] the brush shrinks with increasing salt concentration, but only as a relatively weak power law $c_s^{-1/3}$. There is some experimental and theoretical work that confirms this prediction, but there are other results that are in contradiction. With the new simulation code, we are able to consider systems up to about 7200 charges. This allows studying the effect of additional salt ions. **Fig. 4** shows the brush height as a function of the (free) ion concentration inside the brush for two different grafting densities. Note that this ion concentration is caused by salt co- and counterions and original counterions. Finite size effects have been carefully checked. Finally, we observe an almost perfect agreement with the scaling prediction [6].
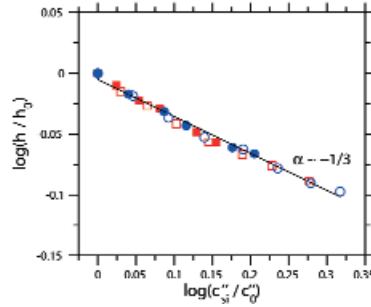

Fig . 4: Brush height as a function the ion concentration inside the brush ($\lambda_B/b = 1$) at grafting density $\rho_a\sigma^2 = 0.04$ (circles) and 0.09 (squares). Simulation results obtained for two different heights of the simulation box: $L_z = 3Nb$ (filled symbols), $L_z = 2Nb$ (open symbols).

Due to the polymer layer close to the anchoring surface, a priori there is a non-homogeneous particle distribution perpendicular to the interface. The first attempt to understand the relation between the concentrations of small ions in the brush and outside the polymer layer at varying salt concentration is by a Donnan equilibrium approach. **Fig. 5** (dashed lines) shows that this fails because of the high concentration in the brush state. However, taking into account the self-volume of PEL chains as indicated above and using the same σ_{eff} we observe a nice agreement with the simulation results for both anchoring densities [6].
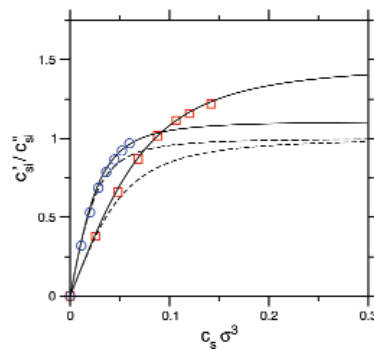

Fig. 5: Relation between the ion concentration inside the brush c_{si}'' and buffer concentration c_{si}' for different salt concentration c_s. Simulation results (symbols as in Fig. 4) and predictions of original (dashed) and modified Donnan approach (solid lines).

C. Seidel, N. A. Kumar, S. Uyaver
Christian.Seidel@mpikg.mpg.de

References:
[1] Uyaver, S. and Seidel, C.: First-order conformational transition of annealed polyelectrolytes in a poor solvent. Europhys. Lett. **64**, 536-542 (2003).
[2] Uyaver, S. and Seidel, C.: Pearl-necklace structures in annealed polyelectrolytes. J. Phys. Chem. B **108**, 18804-18814 (2004).
[3] Uyaver, S. and Seidel, C.: Annealed polyelectrolytes in a poor solvent: effect of varying screening. (in preparation).
[4] Ahrens, H., Förster, S., Helm, C. A., Kumar, N . A., Naji, A., Netz, R. R. and Seidel, C.: Nonlinear osmotic brush regime: experiments, simulations and scaling theory. J. Phys. Chem. B **108**, 16870-16876 (2004).
[5] Pincus, P.: Colloid stabilization with grafted polyelectrolytes. Macromolecules **24**, 2912-2919 (1991).
[6] Kumar, N. A. and Seidel, C.: Polyelectrolyte brushes with added salt. (in preparation).

Structure Formation in Systems of Mesoscopic Rods

Thomas Gruhn 10.06.1969
1995: Diploma, Physics
(Technische Universität Berlin)
Thesis: Monte-Carlo-Untersuchungen
der Ausrichtung nematischer Flüssig-
kristalle (A Monte Carlo study of the
alignment in nematic liquid crystals)
1998: PhD, Physics (Institut für
Theoretische Physik, TU Berlin)
Thesis: Substrate-induced order in
confined molecularly thin liquid-
crystalline films
1999: R&D Project
(Siemens AG, Berlin)
2000: Postdoc
(University of Massachusetts, USA)
2001: Group Leader
(Max Planck Institute for Colloids
and Interfaces, Potsdam)

Mesoscopic structures are a timely research area since new experimental techniques like atomic force microscopy or optical tweezers allow a detailed investigation and manipulation on this length scale. The controlled production of nanostructures on larger scales facilitates the design of new materials, whose mechanical, optical, and chemical properties can be tailored in completely new ways. Inspirations are given from the rich complexity found in molecular cell biology. The controlled production of mesoscopic devices has a wide range of applications reaching from microsurgery, over nanochemistry to a further minimization of microprocessors.

One building block for the creation of nanostructures are mesoscopic rods, which nowadays can be produced in large amounts [1, 2]. With the help of Monte Carlo simulations we investigate how structure formation in systems of mesoscopic rods is influenced by the properties of the molecules and the influence of the environment. The results help to control rod systems in such a way that rodlike macromolecules can be used to build ordered superstructures.

Systems of Chemically Homogenous Rods

Mesoscopic rodlike molecules and molecular assemblies [3] are typically the product of a linear growth process. Therefore, these rods have the same diameter along their axes. For a fluid phase the rods have to be in a solvent. The steric interaction of the rods can be well described by hard spherocylindric rods (*hr*).

Further, attractive interactions may arise from van der Waals and depletion forces. A simplified model for the complete interaction is found by integrating a square well potential along both rod axes. The resulting attractive rod (*ar*) potential can only be calculated with a large numerical effort.

Instead we have developed an angular-dependent site-site potential (see **Fig. 1**) that mimics the ar potential very well with a computational effort comparable to the *hr* potential.
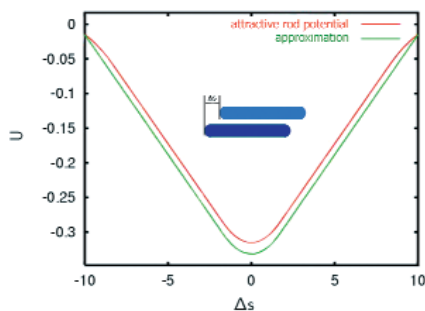
Caused by the production processes, systems of mesoscopic rods typically have a broad length distribution, while for many applications a narrow length distribution would be favorable. A fractionation of rod lengths occurs in the phase coexistence region of the isotropic and a nematic or smectic phase of the system. For the ar potential the formation of an ordered phase occurs at much lower pressures as for the *hr* potential. In an ongoing project, we compare the nucleation behavior of attractive rods with that for hard rods [4].

A binary 1:1 mixture of rods with lengths $L_1=3$ and $L_2=6$ has been investigated in a Gibbs ensemble simulation, in which two simulation boxes are run in parallel [5]. The two boxes can exchange rods and volume such that they have the same pressure and chemical potential. In the phase coexistence region the two sorts of particles demix almost completely. **Fig. 2** shows the two boxes before and after the demixing. The plot in **Fig. 3** illustrates the growing number of small rods and the decreasing number of large rods in box (a). In subsequent simulations the behavior of polydisperse mixtures and the influence of adjacent substrates will be investigated.
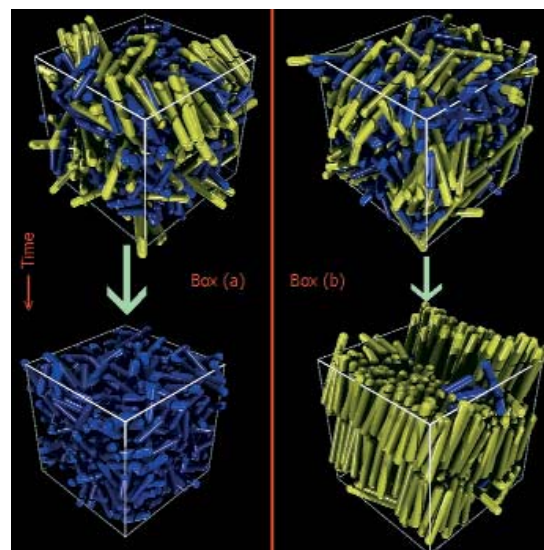

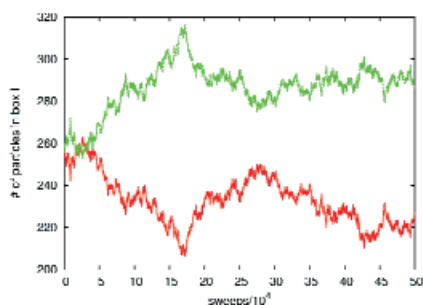*Fig. 2: Demixing of short rods (blue) and long rods (yellow) in a Gibbs ensemble simulation.*

Fig. 1: Attractive rod potential compared with simplified potential.

Fig. 3: Time development of long rods (red) and short rods (green) in box (a).

Systems of Chemically Heterogeneous Rods

Mesoscopically large rods can be tailored to have a chemically heterogeneous structure, which provides new types of ordered structures in the rod system. We investigate hard rods with attractive potentials at the end. In large regions of the phase diagram the behavior of such systems is qualitatively similar to that of systems with chemically homogenous rods. At rather low pressure, however, the formation of a three dimensional, scaffold-like network structure is found showing cluster points where the rods meet with a finite angle (see **Fig. 4**). These structures are stabilized by the addition of an angular dependence of the attractive potential. In a next step we will check if a regular scaffold structure, such as the one shown in **Fig. 5** can be thermodynamically stable with an appropriate potential at the rods' ends.
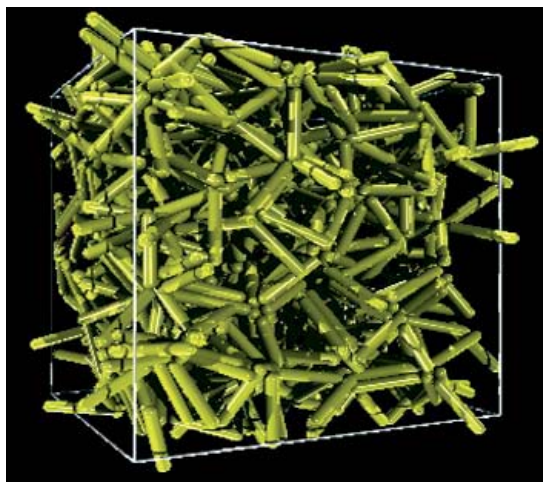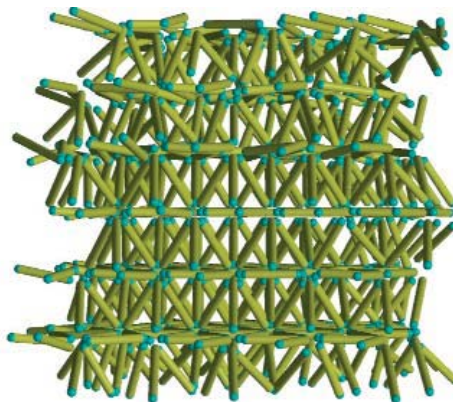

Fig. 5: A scaffold-like fcc-structure is expected to be stable for suitable chemically heterogenous rods.

In another project a system of small rods with attractive ends and long chemically homogenous rods is investigated. This provides a simple model for the cytoskeleton, where the long rods are filaments and the small heterogeneous rods mimic the crosslinkers. Here it will be investigated, how the structure of the filament network depends on the concentration of the crosslinkers.

T. Gruhn, R. Chelakkot, R. Lipowsky, A. Richter
Thomas.Gruhn@mpikg.mpg.de

References:
[1] Schlüter, A.D. and Rabe, J.P.: Dendrinized Polymers: Synthesis, Characterization, Assembly at Interfaces and Manipulation. Angewandte Chemie – International Edition **39**, 864-883 (2000).
[2] van Bruggen, M.P.B. and Lekkerkerker, H. N. W.: Metastability and Multistability: Gelation and Liquid Crystal Formation in Suspensions of Colloidal Rods. Langmuir **18**, 7141-7145 (2002).
[3] Kurth, D.G., Severin, N., and Rabe, J.P.: Perfectly Straight Nanostructures of Metallosupramolecular Coordination-Polyelectrolyte Amphiphile Complexes on Graphite. Angewandte Chemie – International Edition **41**, 3681-3683 (2002).
[4] Schilling, T. and Frenkel, D.: Self-Poisoning of Crystal Nuclei in Hard-Rod Liquids. Physical Review Letters **92**, 085505 (2004).
[5] Richter, A. and Gruhn, T.: Fractionation in mixtures of mesoscopic rods. In preparation.

Fig. 4: Ultraporous structure formed by chemically heterogenous rods with attractive endgroups.

The Elasticity of Silk

Haijun Zhou 04.09.1973
1995: Diploma, Physics
(Nankai University, China)
Thesis: Shape-invariant potentials
in super-symmetric quantum mechanics
2000: PhD, Physics
(Institute of Theoretical Physics, the
Chinese Academy of Sciences, Beijing,
China) Thesis: Elastic and statistical
mechanical theories of polynucleic
acid polymers.
2000-2005: Postdoc
(Max Planck Institute of Colloids
and Interfaces, Potsdam)
2001-2002: Alexander von Humboldt
Research Fellow (Max Planck Institute
of Colloids and Interfaces, Potsdam)
Since 9/2005: Research Professor
(Institute of Theoretical Physics,
Chinese Academy of Sciences,
Beijing, China)

The capture silk of orb weaving spiders is much softer than its dragline silk or the silk for web frame and radii. Nevertheless, its tensile strength per unit weight is still comparable to steel; and unlike steel, the spider capture silk is extremely extensible, being stretchable to almost ten times its relaxed contour length without breaking. This perfect combination of strength and extensibility conveys a high degree of toughness to the capture silk: its rupture energy per unit weight is more than 20 times that of a high-tensile steel.

With the aim to produce synthetic silks with similar mechanical properties, materials scientists have devoted many experimental and computational efforts to the understanding of spider silk's structural organization. Nevertheless, the mechanism behind spider silk's remarkable strength and elasticity is still poorly understood, partly because of the difficulty to obtain high-quality crystallized structures of silk proteins.

Single-molecule force spectroscopy methods were recently applied to spider silks to obtain very detailed information on their force-extension response. Hansma and co-workers attached capture silk mesostructures (probably composed of a single protein molecule) or intact capture silk fibers to an atomic force microscopy tip and recorded the response of the samples to an external stretching force. They found a remarkable exponential relationship between the extension x and the external force f,

$$f \propto \exp\left(x/\ell\right),$$

where ℓ is the length constant; $\ell = 110 \pm 30$ nm for a capture silk molecule and $\ell = 11 \pm 3$ mm for an intact capture silk fiber. This exponential behavior was observed both in solution and in air within a force range from about 10^0 piconewton (pN) to about 10^6 pN.

The exponential force-extension behavior of spider capture silk is significantly different from the force-extension responses of simple biopolymers such as DNA or titin proteins. The elasticity of a simple biopolymer can usually be well predicted by the freely-jointed-chain model or the semiflexible wormlike-chain model. The exponential force extension response of spider capture silk indicates that it is not a 'simple' biopolymer. The question is: Can one infer the structural organization of the spider capture silk from its force-extension response curve?

The exponential force extension response behaviour indicates the following: (1) Because capture silk is highly extensible, a great amount of extra length must have been stored in its relaxed form.

(2) Since extension increases with force logarithmically, some fraction of the stored length can be easily pulled out, a second fraction is more difficult to be pulled out, and a third fraction is even more so etc.

To model this kind of heuristic response cascade, we proposed a *hierarchical chain model* for spider capture silk. In this model, the polymer is composed of many basic structural motifs; these motifs are then organized into a hierarchy, forming structural modules on longer and longer length scales.

At the deepest hierarchy level h_m, the structural motifs could be β-sheets, β-spirals, helices or microcrystal structures. The interactions among some of these motifs are much stronger than their interactions with other motifs, therefore they form a structural module at the hierarchy level (h_m-1).

These level-(h_m-1) modules are then merged into level-(h_m-2) modules through their mutual interactions. This merging process is continued; and finally at the global scale, the whole spider silk string is regarded as a single module of the hierarchy level h=0. We found that the response behavior of such a model polymer is characterized by an exponential force-extension curve.
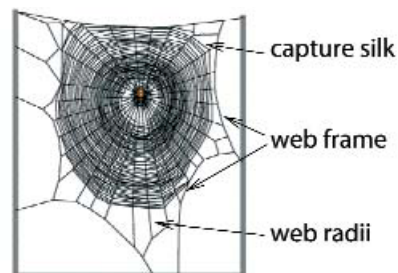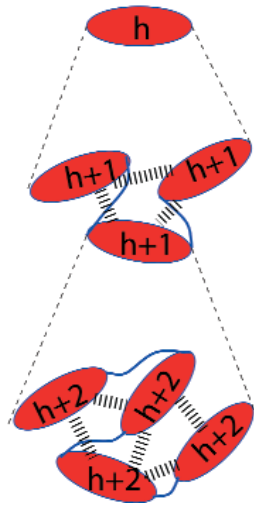

Fig. 1: The web of Araneus diadematus.

Fig. 2: The hierarchical chain model. At each hierarchy level h a structural module M_h is composed of a tandem sequence of m_h submodules M_{h+1} of hierarchy level h+1. Under external stretching, M_h responds by (i) adjusting the arrangements of its m_h subunits and making them more aligned along the force direction, and (ii) extending these m_h subunits. The thick broken lines between submodules of each hierarchy level indicate the existence of sacrificial bonds, such as weak hydrogen bonds or van der Waals attractions.
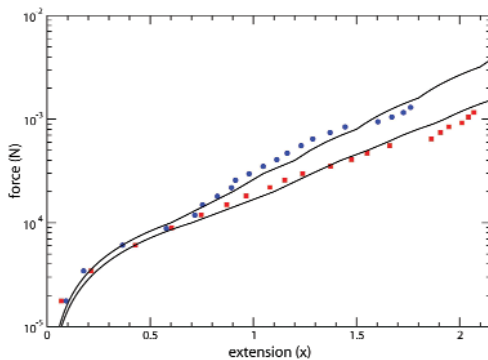

Fig. 3: Exponential force-extension relationship for the hierarchical chain model. Symbols are experimental data from the Hansma group.

Hierarchical chains respond to external perturbations in a hierarchical manner. If the external force is small, only those structural units of length scale comparable to the whole polymer length will be displaced and rearranged; structural units at short and moderate length scales will remain unaffected. As the strength of the external perturbation is increased, additional structural units at shorter length scales are also deformed. Through such a hierarchical organization, a single polymer chain can respond to a great variety of external conditions; at the same time, it is able to keep its structural integrity even under strong perturbations. This hierarchical modular structure also indicates a broad spectrum of relaxation times. The modules at the shorter length scales will have much shorter relaxation times and will be refolded first when the external force decreases. This gap in relaxation times ensures that, after extension, the spider capture silk will return to its relaxed state gradually and slowly. This is a desirable feature for spider capture silk, because a too rapid contraction in response to the insect's impact would propel the victim away from the web.

The simple hierarchical chain model, while appealing, needs further experimental validation. This model seems to be supported by recent genetic sequencing efforts.

H. Zhou
zhou@mpikg.mpg.de

References:

[1] Vollrath, F.: Spider webs and silks, Sci. Am. **266** (3), 70-76 (1992).

[2] Becker, N., Oroudjev, E., Mutz, S., Cleveland, J.P., Hansma, P.K., Hayashi, C.Y., Makarov, D.E. and Hansma, H.G.: Molecular nanosprings in spider capture-silk threads, Nature Materials **2**, 278-283 (2003).

[3] Zhou, H. and Zhang, Y.: Hierarchical chain model of spider capture silk elasticity, Phys. Rev. Lett. **94**, 028104 (2005).

Semiflexible Polymers and Filaments

Jan Kierfeld 31.01.1969
1993: Diploma, Physics
(Universität zu Köln)
Thesis: Zur Existenz der Vortex-
Glas-Phase in Schichtsystemen
1995-1996: Research Associate
(UC San Diego)
1996: PhD, Physics
(Universität zu Köln)
Thesis: Topological Order and Glassy
Properties of Flux Line Lattices in
Disordered Superconductors
1997-2000: Postdoc
(Argonne National Laboratory)
Since 2000: Group Leader,
(Max Planck Institute of Colloids
and Interfaces, Potsdam)

Many biopolymers such as DNA, filamentous (F-) actin or microtubules belong to the class of semi-flexible polymers. The biological function of these polymers requires considerable mechanical rigidity. For example, actin filaments are the main structural element of the cytoskeleton which gives the cell unique mechanical properties as it forms a network rigid enough to maintain the shape of the cell and to transmit forces, yet flexible enough to allow for cell motion and internal reorganization in response to external mechanical stimuli. Another important class of semi-flexible polymers are polyelectrolytes where the electrostatic repulsion of the charges along the backbone can give rise to considerable bending rigidity depending on the salinity of the surrounding solution.

The physics of semi-flexible polymers becomes fundamentally different from the physics of flexible synthetic polymers when their bending energy dominates over conformational entropy. The bending stiffness is characterized by the persistence length. On scales smaller than the persistence length, bending energy dominates and qualitatively new semi-flexible behaviour appears. Biopolymer persistence lengths range from 50nm for DNA to the 10μm-range for F-actin or even up to the mm-range for microtubules and are thus comparable to typical contour lengths such that semi-flexible behaviour plays an important role.

Binding and Adsorption

Binding of two polymers and adsorption of a polymer onto a surface **(Fig. 1)** are two phase transitions of fundamental importance. For both transitions, semi-flexibility is relevant and leads to new critical exponents, or changes even the order of the transition **[1,2]**. In contrast to flexible polymers, binding and adsorption transitions of semiflexible polymers are typically *discontinuous*. Semiflexible polymers bind or adsorb more easily the more rigid they are.

Fig.1: Left: Binding of two polymers, Right: Adsorption onto an adhesive surface.

Single Polymer Manipulation

During the last decade micromanipulation techniques such as optical tweezers and atomic force microscopy (AFM) have become available which allow a controlled manipulation of single polymers and filaments. Experiments such as stretching of single DNA polymers or pushing adsorbed polymers over a surface with an AFM tip open up the possibility of characterizing mechanical filament properties on the single molecule level. In order to interpret experiments quantitatively, theoretical models are necessary which allow to calculate the response of a polymer to external forces. We investigated such models for (i) the stretching of semiflexible harmonic chains **[3]**, (ii) the activated dynamics of semiflexible polymers on structured substrates **[4,5]**, and (iii) force-induced desorption.

(i) In order to improve the quantitative interpretation of force-extension curves from stretching experiments on single semiflexible polymers such as DNA or F-actin, we introduced a semiflexible harmonic chain model **[3]**. This model includes not only the bending rigidity, but also takes into account the polymer extensibility, the monomer size and the finite contour length. Our results for this model allow to extract all of these parameters from experimental force-extension curves. (ii) Strongly adsorbed polymers are often subject to surface potentials that reflect the symmetry of the underlying substrate and tend to align in certain preferred directions. If such polymers are pushed over the substrate by a homogeneous force arising, e.g., from hydrodynamic flow or by a point force as can be exerted by AFM tips, their dynamics is thermally activated and governed by the crossing of the surface potential barriers. Barrier crossing proceeds by nucleation and subsequent motion of kink-antikink pairs **(Fig. 2)**. The analysis of this process shows that static and dynamic kink properties are governed by the bending rigidity of the polymer and the potential barrier height **[4,5]**, which implies that experimental measurements of the kink properties can be used to characterize material properties of both the semiflexible polymer and the substrate.
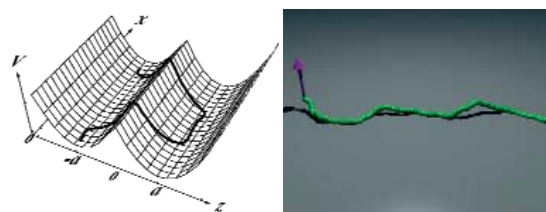

Fig. 2: Left: Kinked conformation of a semi-flexible polymer in a double-well potential. Right: Snapshot of a Monte-Carlo simulation of an adsorbed polymer. A force applied to one polymer end (arrow) can lead to force-induced desorption

(iii) AFM tips can also be used to lift an adsorbed polymer from a surface **(Fig. 2)**. We can calculate the resulting force-extension characteristics for such a force-induced desorption process. One interesting feature is the occurrence of an energetic barrier against force-induced desorption which is solely due to the effects from bending rigidity.

Filament Bundles

Filament assemblies play an important role as functional and structural elements of the cytoskeleton. Using analytical and numerical methods we studied the formation of filament bundles. In the cell, filament bundles are held together by adhesive crosslinking proteins. In a solution of crosslinkers and filaments, the crosslinkers induce an effective attraction between filaments. Starting from analytical results for two filaments **[1,2]**, we have studied this problem analytically for N filaments and numerically for up to 20 filaments using Monte-Carlo simulations **[6]**. Above a threshold concentration of crosslinkers a bundle forms in a discontinuous bundling phase transition **[6]**. This mechanism can be used by the cell to regulate bundle formation. Deep in the bundled phase at high crosslinker concentration, we observe a segregation of bundles into smaller sub-bundles, which are kinetically arrested **(Fig. 3)**. The system appears to be trapped in a glass-like state. Starting from a compact initial state, on the other hand, the bundle reaches its equilibrium configuration with a hexagonal arrangement of filaments **(Fig. 3)**.
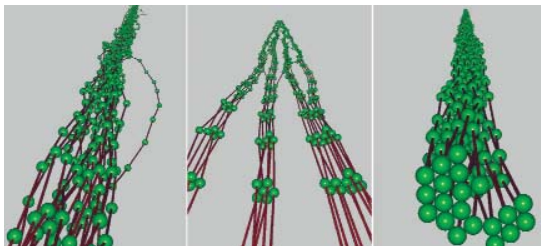

Fig. 3: Monte-Carlo snapshots of filament bundles.
Left: Close to the bundling transition.
Middle: Deep in the bound phase bundles tend to segregate.
Right: Equilibrium shape of the bundle.

Active Filaments

The living cell is an active system where cytoskeletal filaments are not in equilibrium. ATP- or GTP-hydrolysis allows them to constantly polymerise and de-polymerise (treadmilling). The active polymerisation dynamics can be used for force generation. Extending our work on filament bundles, we study force generation by growing filament bundles.

Cytoskeletal filaments not only generate force by active polymerisation but also interact with molecular motors, which are motor proteins walking on filaments by converting chemical energy from ATP-hydrolysis into mechanical energy. The interplay between filaments and molecular motors can give rise to structure formation far from equilibrium. This can be studied in model systems such as motility assays where filaments are adsorbed and actively transported over a glass plate, which is covered with anchored molecular motors. Computer models of such assays allow to predict and quantify formation of filament patterns, e.g., clustering and ordering **(Fig. 4)**. Apart from motor and filament densities, also microscopic motor parameters such as their stall and detachment force determine the emerging pattern and can thus be inferred from the experimentally observed filament structures.
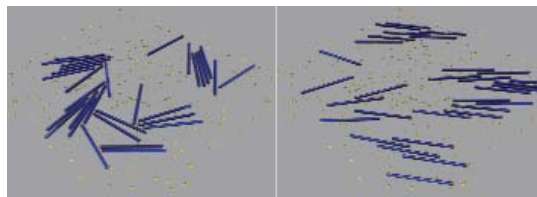

Fig. 4: Snapshot of a motility assay simulation. Filaments (blue) are driven by molecular motors (yellow) over a substrate (grey).
Left: Formation of immobile clusters of filaments blocking each other.
Right: Nematic ordering due to collisions of moving filaments.

J. Kierfeld, P. Kraikivski, T. Kühne, R. Lipowsky
kierfeld@mpikg.mpg.de

References:
[1] Kierfeld, J. and Lipowsky, R.: Unbundling and desorption of semiflexible polymers, Europhys. Lett. **62**, 285-291 (2003).
[2] Kierfeld, J. and Lipowsky, R.: Duality mapping and unbinding transitions of semiflexible and directed polymers, J. Phys. A: Math. Gen., **38**, L155-L161 (2005).
[3] Kierfeld, J., Niamploy, O., Sa-yakanit, V. and Lipowsky, R.: Stretching of Semiflexible Polymers with Elastic Bonds, Eur. Phys. J. E **14**, 17-34 (2004).
[4] Kraikivski, P., Lipowsky, R. and Kierfeld, J.: Barrier crossing of semiflexible polymers, Europhys. Lett. **66**, 763-769 (2004).
[5] Kraikivski, P., Lipowsky, R. and Kierfeld, J.: Activated dynamics of semiflexible polymers on structured substrates, Eur. Phys. J. E, in press (2005).
[6] Kierfeld, J., Kühne, T. and Lipowsky, R.: Discontinuous unbinding transitions of filament bundles, submitted to Phys. Rev. Lett. (2004).

Traffic of Molecular Motors

Stefan Klumpp 29.09.1973
1999: Diploma, Physics
(University of Heidelberg)
Thesis: Noise-induced transport
of two coupled particles
2003: PhD, Physics
(Max Planck Institute of Colloids
and Interfaces, Potsdam)
Thesis: Movements of molecular
motors: Diffusion and directed walks
Since 2004: Group Leader
(Max Planck Institute of Colloids
and Interfaces, Potsdam)

Molecular motors are proteins which catalyze a chemical reaction and use the free energy released from this reaction to generate directed movements and to perform work. Examples are the cytoskeletal motors which move in a directed fashion along cytoskeletal filaments, e.g. kinesins which move along microtubules. They consume adenosinetriphosphate (ATP) which represents their chemical 'fuel' and move in discrete steps in such a way that one molecule of ATP is used per step. Our understanding of molecular motors is based on biomimetic model systems which are rather simple compared to biological cells and consist of only a small number of components such as motors, filaments, and ATP. These systems allow us to study the transport properties of molecular motors systematically. A typical biomimetic experiment is shown in **Fig. 1**.
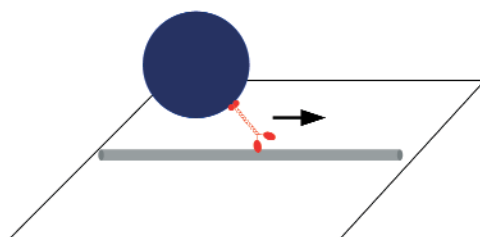

Fig. 1: The bead assay provides an example for a biomimetic model experiment: A molecular motor transports a (glass or latex) bead along a filament which is immobilized on a surface.

Unbinding and Motor Walks

A molecular motor is called processive if it makes many steps while it is bound to the filament. However, even processive motors have only a finite walking distance, because the motor-filament binding energy can be overcome by thermal fluctuations. This walking distance is typically of the order of 1 µm for cytoskeletal motors. Unbound motors perform Brownian motion in the surrounding aqueous solution until they collide again with a filament and rebind to it.

Therefore, on large length and time scales which exceed a few microns and a few seconds, respectively, molecular motors perform peculiar motor walks as shown in **Fig. 2**. These motor walks consist of alternating sequences of active directed movements along filaments and passive non-directed diffusion [1].
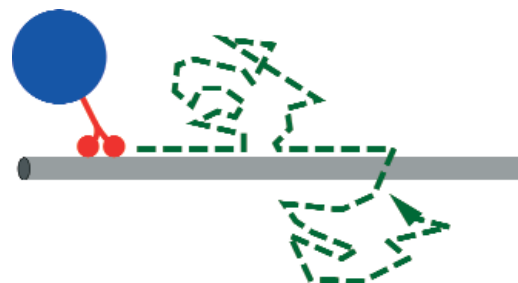

Fig. 2: Motor walks: A molecular motor performs active directed movement along a filament and unbinds from it after a certain walking distance. The unbound motor diffuses passively in the surrounding fluid until it rebinds to the filament and resumes directed motion.

We have studied these motor walks for various compartments with different geometries using both computer simulations and analytical techniques [1, 2]. The motor walks exhibit anomalous drift behaviour and strongly enhanced effective diffusion due to the repeated binding to the filament. The enhanced diffusion is particularly pronounced if the walking distance is large, which is the case for motor particles driven by several motor molecules.

Exclusion and Jamming

If the concentration of molecular motors in a compartment is large, motor-motor interactions become important and lead to a variety of cooperative phenomena. In particular, motors interact via simple exclusion or hard core repulsion which implies that a motor bound to a binding site of the filament excludes other motors from this filament site. This type of motor-motor interaction leads to traffic jams on the filament and implies the existence of various kinds of phase transitions. In contrast to the traffic of cars and other vehicles, unbinding from the filament and diffusion of unbound motors play a role in the traffic of molecular motors. We have focussed on tube-like compartments as shown in **Fig. 3** with different kinds of boundary conditions. The tube geometry mimics the geometry of an axon, which provides the most prominent example for long-range motor traffic in vivo.

(a)

(b)

$\rho_b \ell^3$
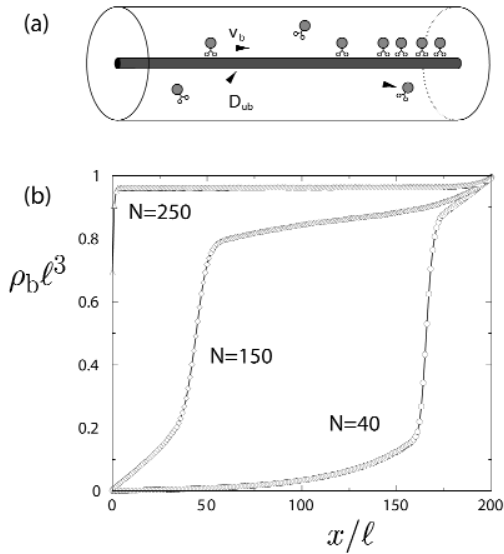
N=250

N=150

N=40

x/ℓ

Fig. 3: (a) Motors move in a closed tube system which contains one filament and build up a motor traffic jam at the right end of the system. (b) Profiles of the bound motor density along the filament for various total numbers N of motors within the tube. The jammed region becomes longer with increasing N.

In closed tubes, the motors generate non-uniform density patterns and accumulate at the end of the tubes as shown in **Fig. 3**. The average bound motor current in these systems exhibits a maximum as a function of the motor concentration within the tube [1].

Open tube systems, which are coupled to motor reservoirs at both ends, exhibit boundary-induced phase transitions [3]. The motor density within the tube is determined by the 'bottleneck' of the transport through the tube, which can be given by one of the boundaries or by the interior of the tube. Phase transitions occur if the position of the 'bottleneck' changes when the motor densities in the boundary reservoirs are changed.

Bidirectional Motor Traffic

Each molecular motor moves either towards the plus- or towards the minus-end of the corresponding filament, but different types of motors move into opposite directions along the same filament. In this situation, cooperative binding of the motors to the filament—in such a fashion that a motor is more likely to bind next to a bound motor moving in the same direction and less likely to bind next to a motor with opposite directionality—leads to spontaneous symmetry breaking [4]: For sufficiently strong motor-motor interactions, one motor species occupies the filament, while the other one is largely excluded from it as shown in **Fig. 4**. If several filaments are aligned in parallel and with the same orientation, this symmetry breaking leads to the spontaneous formation of traffic lanes for motor traffic with opposite directionality [4].
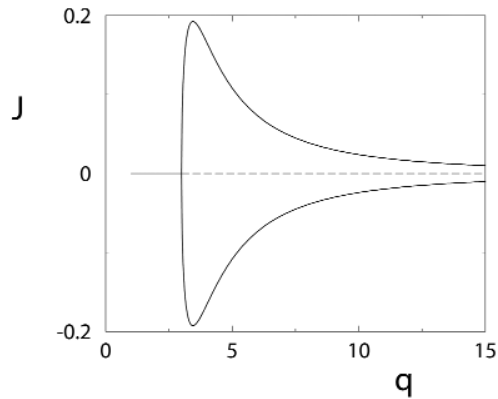

Fig. 4: Spontaneous symmetry breaking in systems with two motor species moving into opposite directions along the same filament: The total motor current J is zero for weak interaction $q<q_c$, where the filament is equally populated by both motor species, but non-zero for sufficiently strong motor-motor interactions with $q>q_c$, where one motor species is essentially excluded from the filament. For very strong interaction, the current decreases because the filament becomes more and more crowded.

S. Klumpp, Y. Chai, R. Lipowsky, M. Müller
klumpp@mpikg.mpg.de

References:
[1] Lipowsky, R., Klumpp, S. and Nieuwenhuizen, T.M.: Random walks of cytoskeletal motors in open and closed compartments. Phys. Rev. Lett. **87**, 108101/1-4 (2001).
[2] Nieuwenhuizen, T.M., Klumpp, S. and Lipowsky, R.: Random walks of molecular motors arising from diffusional encounters with immobilized filament. Phys. Rev. E **69**, 061911/1-19 (2004).
[3] Klumpp, S. and Lipowsky, R.: Traffic of molecular motors through tube-like compartments. J. Stat. Phys. **113**, 233-268 (2003).
[4] Klumpp, S. and Lipowsky, R.: Phase transitions in systems with two species of molecular motors. Europhys. Lett. **66**, 90-96 (2004).

Protein Folding

Thomas Weikl 01.04.1970
1996: Diploma, Physics
(Freie Universität Berlin)
Thesis: Interactions of rigid
membrane inclusions
1999: PhD, Physics
(Max Planck Institute of Colloids
and Interfaces, Potsdam)
Thesis: Adhesion of
multicomponent membranes
2000-2002: Postdoc
(University of California,
San Francisco)
Since 2002: Group Leader
(Max Planck Institute of Colloids
and Interfaces, Potsdam)

Since their discovery about 10 years ago, two-state folders constitute a new paradigm in protein folding. Two-state folders are proteins that fold from the denatured state to the native state highly cooperatively, without experimentally detectable intermediate states. Most of the small single-domain proteins characterized to date fold with two-state kinetics. These single domains are also thought to build the folding units of the larger and more complex multi-domain proteins.

The central experimental tool for investigating the folding kinetics of two-state proteins is mutational analysis. A careful mutational analysis requires generating a large set of single-residue mutants of the considered protein. The impact of each of these mutations on the folding kinetics is then typically characterized by the Φ-value, defined as

$$\Phi = \frac{RT\ln\left(k_{wt}/k_{mut}\right)}{\Delta G_N}$$

Here, k_{wt} and k_{mut} represent the folding rates of the wildtype and mutant of the protein, and ΔG_N is the change in stability induced by the mutation. The stability of a protein is the free energy difference between the denatured state D and the native state N.

Two-state folding is often described in transition-state theory, which assumes that the folding rate is proportional to exp(-G_T/RT). Here, G_T is the activation energy of the folding reaction, the free energy difference between the rate-limiting transition-state ensemble T and the denatured state D. This implies $\Phi = \Delta G_T / \Delta G_N$, which indicates that Φ-values measure the *energetic* consequences of mutations on the transition state ensemble relative to the native state.

A central question is whether Φ-values also contain *structural* information about the transition state ensemble. In the traditional interpretation, Φ=1 is taken to indicate that the mutated residue has native-like structure in the transition state ensemble, since the mutation-induced free energy shifts of the transition state ensemble and the native state, ΔG_T and ΔG_N, are equal. Oppositely, Φ=0 is taken to indicate that the mutated residue is not structured in the transition-state ensemble. Most of the mutations have 'fractional' Φ-values between 0 and 1, which apparently indicates a partially native-like structural character of the mutated residue in the transition state ensemble. However, there are several problems with this traditional structural interpretation. For example, Φ-values are sometimes 'nonclassical', i.e. they can be less than zero or larger than one. In the traditional view, such values cannot be interpreted.

We have recently developed a more rigorous interpretation of Φ-values [5]. In this interpretation, Φ-values have both *structural and energetic* components. The interpretation is based on a statistical-mechanical model that focuses on the formation of characteristic protein substructures during folding. The model describes the folding kinetics *via* a master equation which can be solved exactly [3,5]. In the model, Φ-values for mutations in an α-helical substructure with intrinsic stability G_α have the general form

$$\Phi = \chi_\alpha \frac{\Delta G_\alpha}{\Delta G_N}$$

Here, χ_α is a *structural* term between 0 and 1, indicating to which extent the α-helix participates in the transition state ensemble. The *energetic* term $\Delta G_\alpha / \Delta G_N$ can attain any value and can thus lead to nonclassical Φ-values smaller than 0 or larger than 1.

The protein Cl2 (see **Fig. 1**) is one of the best-characterized two-state folders. The Φ-values for 20 single-residue mutations in the α-helix of Cl2 range from −0.35 to 1.25. Our model reproduces these Φ-values with a correlation coefficient of 0.85, including several of the nonclassical Φ-values, and provides a consistent structural interpretation of these values [5].
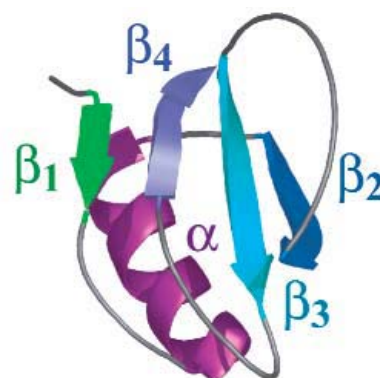

Fig 1: The protein Cl2 is one of the best-characterized two-state folders. The structure of Cl2 consists of an α-helix packed against a four-stranded β-sheet.

Another important question is why some proteins have *polarized* Φ-value distributions, while others have *diffuse* distributions. In a polarized distribution, the Φ-values in some of the secondary structural elements (helices or strands) of the protein are significantly larger than in other secondary elements. In a diffuse distribution, the average Φ-values for the secondary structural elements of the protein are rather similar.

We have found that the shape of many Φ-value distributions can be understood from loop-closure events during folding [1, 2, 4]. The loops of the protein chain closed during folding depend on the sequences of events in which the structural elements are formed (see **Fig. 2**).
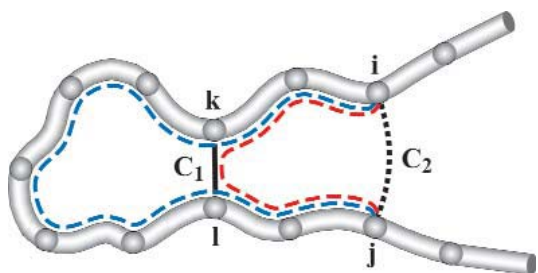
Fig. 2: Loop-closure dependencies between contacts. Forming contact C_2 prior to C_1 requires the closure of a relatively large loop (blue line). But if the contact C_1 closes first, the loop for forming C_2 is significantly smaller (red line).

On the minimum-entropy-loss routes of our models, the structural elements of the protein 'zip up' in a sequence of events that involves only relatively small loops (see **Fig. 3**). The 'kinetic impact' of the structural elements estimated from these routes correlates with the average experimental Φ-values [4]. A structural element that strongly affects the loop lengths for forming other structural elements is predicted to fold early and to have a high kinetic impact in this model.
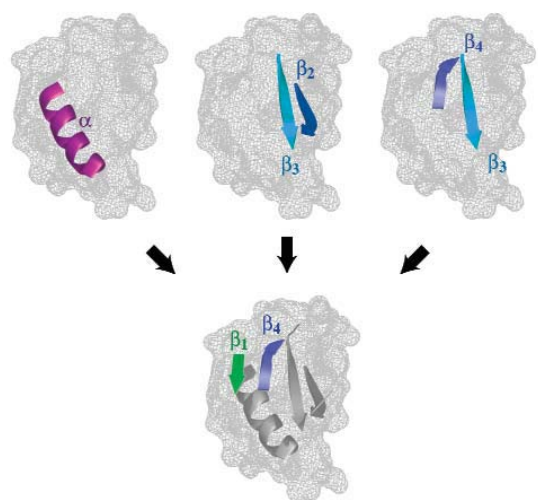
A third question currently addressed by us concerns the multiplicity of protein folding routes. According to the 'old view', proteins fold along well-defined sequential pathways, whereas the 'new view' sees protein folding as a highly parallel stochastic process on funnel-shaped energy landscapes. We have analyzed parallel and sequential processes on a large number of Molecular Dynamics unfolding trajectories for the protein CI2 at high temperatures [6]. Using statistical measures, we find that the degree of sequentiality depends on the structural level under consideration. On a coarse structural level of whole β-sheets and helices, unfolding is predominantly sequential. In contrast, the unfolding process is highly parallel on the level of individual contacts between the residues of the protein chain. On an intermediate structural level, the characteristic parallel and sequential events during unfolding can be understood from the loop-closure dependencies between the structural elements.

T. R. Weikl, C. Merlo, L. Reich
thomas.weikl@mpikg.mpg.de

References:
[1] Weikl, T.R., and Dill, K.A.: Folding rates and low-entropy-loss routes of two-state proteins. J. Mol. Biol. **329**, 585-598 (2003).
[2] Weikl, T.R., and Dill, K.A.: Folding kinetics of two-state proteins: Effect of circularization, permutation, and cross-links. J. Mol. Biol. **332**, 953-963 (2003).
[3] Weikl, T.R., Palassini, M., and Dill, K.A.: Cooperativity in two-state protein folding kinetics. Protein Sci. **13**, 822-829 (2004).
[4] Weikl, T.R.: Loop-closure events during protein folding: Rationalizing the shape of Φ-value distributions. Proteins, in press
[5] Merlo, C., Dill, K.A, and Weikl, T.R.: Φ-values in protein folding kinetics have energetic and structural components. Submitted
[6] Reich, L., and Weikl, T.R.: How parallel is protein (un)folding? In preparation

Fig. 3: Minimum-entropy-loss route for the protein CI2. Along this route, the nonlocal pairing of the terminal strands β_1 and β_4 is formed after the α-helix and after the local strand pairings $\beta_2\beta_3$ and $\beta_3\beta_4$. The prior formation of the three local structural elements reduces the length of the loop which has to be closed to form $\beta_1\beta_4$.

BIOLOGICAL SYSTEMS

Emmy Noether Junior Research Group
Cellular Adhesion Clusters under Force

Dr. Ulrich Schwarz 03.03.1966
1994: Diploma, Physics
(Ludwig Maximilians University Munich)
Thesis: Structure Formation in Binary
Amphiphilic Systems
1998: PhD, Physics
(Max Planck Institute of Colloids
and Interfaces, Potsdam and
Potsdam University)
Thesis: Mesoscopic Modelling
of Amphiphilic Systems
1998-2000: Postdoc
(Weizmann Institute, Rehovot, Israel)
2000-2001: Group Leader
(Max Planck Institute of Colloids
and Interfaces, Potsdam)
2001-2005: Leader of an Emmy
Noether Junior Research Group
(Max Planck Institute of Colloids
and Interfaces, Potsdam)
2004: Habilitation, Theoretical Physics
(Potsdam University) Thesis: Forces
and Elasticity in Cell Adhesion
Since 2005: Leader of a Junior
Research Group in the Centre for
Modelling and Simulations in the
Biosciences (BIOMS, Heidelberg
University)

Physical concepts are essential to understand the functioning of biological cells. For example, the physical properties of cytoskeleton, plasma membrane, adhesion clusters and extracellular matrix strongly influence cell shape, adhesion and migration, which in turn are essential elements of many important physiological processes, including development, inflammation and wound healing. During recent years, a large variety of new experimental tools has been developed in biophysics and materials science which now allow to characterize and control various physical determinants of cellular systems in a quantitative way. On the extracellular side, this includes the use of soft lithography to create biochemically, topographically and mechanically structured surfaces. On the intracellular side, this includes a large variety of novel fluorescence probes, colloidal spectroscopy and microrheology. In parallel to these experimental advances, concepts from statistical mechanics and soft matter physics have been increasingly applied to cellular systems.

In cell adhesion, physical concepts like force and elasticity are particularly important. Cells adhere to each other and to the extracellular matrix through clusters of transmembrane adhesion receptors, which on the intracellular side usually couple to the cytoskeleton. Therefore they usually are under considerable mechanical load. For example, adherens junctions in cell-cell adhesion and focal adhesions in cell-matrix adhesion are mediated by receptors from the cadherin and integrin families, respectively, which both couple to the actin cytoskeleton. In some cases, cell adhesion is determined by the interplay between several receptor systems. One example is the way in which white blood cells, but also stem and cancer cells exit the blood flow, as depicted schematically in **Fig. 1**. In the initial stages, the white blood cells bind to the vessel walls through receptors from the selectin family. Because the selectin bonds break rapidly, the cells start to roll, with new bonds forming at the front and old ones breaking at the back. The main function of rolling adhesion is to slow down the cell in such a way that it can survey the vessel walls for exit signals. If these are present, firm adhesion through long-lived integrin receptors is activated, leading to arrest and subsequent extravasation from the blood vessel. Thus rolling adhesion is characterized by the interplay of selectin and integrin receptors, which both couple to the actin cytoskeleton.

The coupling of adhesion clusters to the cytoskeleton does not only provide structural integrity, it also allows the cell to regulate the internal state of the adhesion cluster by force. For example, it has been shown during recent years that focal adhesion act as mechanosensors, i.e. they convert force into intracellular signalling events **[1,2]**. Mechanical properties of the extracellular environment modulate the build-up of actomyosin-generated force at focal adhesions and therefore can be sensed by cells through force-mediated processes at focal adhesion. Based on this information, cells can for example decide how to position and orient in a mechanically anisotropic environment **[3,4]**.
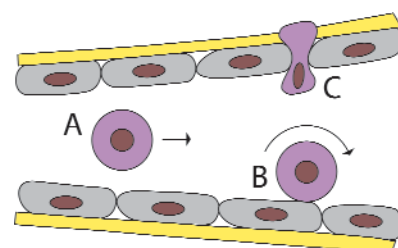

Fig. 1: White blood cells, but also stem and cancer cells travel the body in the blood flow (A). In order to exit the blood flow, they have to interact adhesively with the vessel walls. Initial adhesion is provided by short-lived selectin-bonds, resulting in rolling adhesion (B). Adhesion through long-lived integrin-bonds leads to firm arrest and extravasation (C).

Stochastic Dynamics of Adhesion Clusters

In order to understand these processes in more detail, microscopic models for force-modulated processes at adhesion clusters are required. In general, formation and rupture of adhesion bonds is a stochastic process. In this context, the simplest theoretical model for a biomolecular bond is a one-dimensional energy landscape with a transition state barrier separating the unbound from the bound state. Then the average bond lifetime T_0 can be identified with the mean first passage time to cross the transition state barrier. Kramers theory predicts that T_0 is an exponential function of barrier height in units of thermal energy. The resulting values for T_0 are typically of the order of seconds. Force tilts the energy landscape. For a sharp transition state barrier, Kramers theory predicts that average bond lifetime T under force decreases in an exponential way as function of force, $T = T_0 \, e^{-f}$, where f is force in units of thermal energy divided by the distance between the bound state and the sharp transition state barrier. The resulting intrinsic force scale typically is of the order of pico-Newtons. In 1978, Bell postulated this relation for single bonds under constant force. In 1997, Evans and Ritchie applied this concept to single bonds under time-dependent forces. They predicted that for a linearly rising force, average bond lifetime becomes a logarithmic function of loading rate. This prediction has been confirmed impressively in subsequent experiments and defined the new field of *dynamic force spectroscopy*. Since force is usually applied through some soft transducer, the bond cannot rebind after rupture due to elastic recoil of the transducer.

Since adhesion bonds in cellular systems usually act in a cooperative way in adhesion clusters, this single molecule effort now has to be extended to multiple bonds. In contrast to the situation with single bonds, now rebinding should be possible as long as at least one closed bonds can ensure spatial proximity of receptors and ligands. In order to investigate the role of force for the stochastic dynamics of adhesion clusters, we studied a one-step master equation for the dynamics of N parallel adhesion bonds under dimensionless force f and with dimensionless rebinding rate γ **[5,6]**. **Fig. 2** schematically shows the situation under consideration. In our model, we neglect spatial aspects and the state of the adhesion cluster is described completely by the number i of closed bonds. There are N+1 possible states ($0 \leq i \leq N$) and the

reverse and forward rates between the different state are $i\,e^{f/i}$ and $\gamma(N-i)$. Here the factor f/i reflects the fact that force is assumed to be shared equally between the closed bonds, leading to non-trivial cooperativity between the different bonds. For finite force, this model is highly non-linear and therefore difficult to solve. Nevertheless exact solutions can be found for several special cases, including $f=0$, $\gamma=0$ and $N=2$. In the general case of arbitrary N, f and γ, the master equation can be solved by computer simulations, for example by adapting the Gillespie algorithm for exact stochastic simulations. Computer simulations are also essential to reveal the nature of single rupture trajectories. For most of the time, these trajectories follow the smooth time course of the first moment. The final stages of rupture however are characterized by rather abrupt decay which results from the Arrhenius factor $e^{f/i}$ in the reverse rate: if the number of closed bonds i fluctuates to a smaller value, force on the remaining closed bonds and therefore their dissociation rate increase, leading to a positive feedback loop for rupture. Our analysis also shows that there is a threshold in force beyond which rupture is increased strongly. Moreover our master equation can be used to study the case of a linearly rising force [7], a situation which is relevant for dynamic force spectroscopy on adhesion clusters.
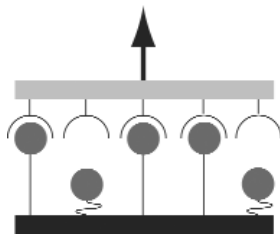

Fig. 2: Schematic representation of an adhesion cluster under force: in this cartoon, there are N=5 identical receptor-ligand bonds, of which i=3 are closed and equally share the dimensionless force f. At the same time, N-i=2 bonds are open and can rebind with the dimensionless rebinding rate γ.

For experimental purposes, the quantity of largest interest is the average cluster lifetime T as a function of the model parameters N, f and γ. This quantity can be identified with the mean first passage time to reach the completely dissociated state. For constant force, it can be calculated exactly from the adjoint master equation for arbitrary model parameters. In the case N=2, we find

$$T = \frac{T_0}{2}\left(e^{-f/2} + 2e^{-f} + \gamma e^{-3f/2}\right).$$

This two-bond equation can be understood as the generalization of Bell's single bond equation $T = T_0\, e^{-f}$. For arbitrary N, we find that average cluster lifetime T is always exponentially suppressed by force f and that the stabilizing contribution due to rebinding is a polynomial in γ of rank N-1.

Adhesion Clusters in Rolling Adhesion

In a collaboration with immunologists from the Weizmann Institute in Israel, we used these results to evaluate flow chamber data for white blood cells adhering under shear flow [8,9]. The red line with circles in **Fig. 3** shows the measured dissociation rate as a function of shear rate for single cells transiently tethered to the bottom of the flow chamber sparsely coated with ligands for L-selectin. At low shear, the dissociation rate plateaus at a value of 250 Hz, which most likely is the intrinsic dissociation rate of single L-selectin bonds. The force acting on the cell due to viscous drag from the hydrodynamic flow can be calculated from the Stokes equation. Combined with Bell's equation, this leads to the light blue line in **Fig. 3**, which clearly does not agree with the experimental data. However, this calculation neglects the fact that at low shear, both intrinsic dissociation and loading occur on the same time scale of milliseconds. Correcting Bell's equation for initially linear loading leads to the green line in **Fig. 3**, which is much closer to the experimental result. Most importantly, **Fig. 3** shows that at a shear rate of 40 Hz, the cellular dissociation rate suddenly drops by a factor of 14. This dramatic stabilization can be argued to result from multiple bond formation due to increased transport at higher shear. Several lines of reasoning suggest that the dominating event is the formation of two-bond clusters. The dark blue lines in **Fig. 3** are plots of the two-bond equation for different values for the rebinding rate γ. The value $\gamma=40$ (10^4 Hz in dimensional units) agrees best with the experimental data, suggesting that L-selectin mediated tethering in shear flow is characterized by unusual fast rebinding. Although these results represent only a small step toward a complete understanding of the complicated process of rolling adhesion, they show how quantitative evaluation of experimental data can help to dissect complex cellular systems.
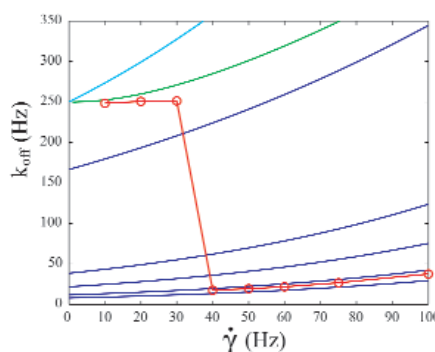

Fig. 3: Red line with circles: experimental data for cellular dissociation rate as a function of shear rate as measured in flow chambers for white blood cells adhering through L-selectin. Light blue line: single bond dissociation as predicted by Bell's equation with immediate loading. Green line: Bell's equation corrected for finite loading rate. Dark blue lines: two-bond equation for different values of the rebinding rate γ (γ=0, 10, 20, 40 and 60 from top to bottom). Agreement with the experimental data is best for γ=40.

U. Schwarz, I. Bischofs, T. Erdmann, C. Korn
Ulrich.Schwarz@iwr.uni-heidelberg.de

References:

[1] Balaban, N.Q., Schwarz, U.S., Riveline, D. Goichberg, P., Tzur, G. , Sabanay, I., Mahalu, D., Safran, S., Bershadsky, A., Addadi, L. and Geiger, B.: Force and focal adhesion assembly: a close relationship studied using elastic micro-patterned substrates. Nat. Cell Biol. **3**, 466-472 (2001).

[2] Riveline, D., Zamir, E., Balaban, N. Q., Schwarz, U.S., Geiger, B., Kam, Z. and Bershadsky, A. D.: Focal contact as a mechanosensor: externally applied local mechanical force induces growth of focal contacts by a mDia1-dependent and ROCK-independent mechanism. J. Cell Biol. **153**, 1175-1185 (2001).

[3] Bischofs, I.B. and Schwarz, U.S.: Cell organization in soft media due to active mechanosensing. Proc. Natl. Acad. Sci. USA **100**, 9274-9279 (2003).

[4] Bischofs, I.B., Safran, S.A. and Schwarz, U.S.: Elastic interactions of active cells with soft materials. Phys. Rev. E **69**, 021911 (2004).

[5] Erdmann, T. and Schwarz, U.S.: Stability of adhesion clusters under constant force. Phys. Rev. Lett. **92**, 108102 (2004).

[6] Erdmann, T. and Schwarz, U.S.: Stochastic dynamics of adhesion clusters under shared constant force and with rebinding. J. Chem. Phys. **121**, 8997-9017 (2004).

[7] Erdmann, T. and Schwarz, U.S.: Adhesion clusters under shared linear loading: a stochastic analysis. Europhys. Lett. **66**, 603-609 (2004).

[8] Dwir, O., Solomon, A., Mangan, S., Kansas, G.S., Schwarz, U.S. and Alon, R.: Avidity enhancement of L-selectin bonds by flow: shear-promoted rotation of leukocytes turn labile bonds into functional tethers. J. Cell Biol. **163**, 649-659 (2003).

[9] Schwarz, U.S. and Alon, R.: L-selectin mediated leukocyte tethering in shear flow is controled by multiple contacts and cytoskeletal anchorage facilitating fast rebinding events. Proc. Natl. Acad. Sci. USA **101**, 6940-6945 (2004).

Evolution in Stochastic Environments

Angelo Valleriani 14.03.1966
1992: Diploma, Physics
(University of Bologna)
Thesis: Conformal Invariance,
Renormalization Group and Integrable
Models in Two-Dimensional Quantum
Field Theories
1996: PhD, High-Energy Physics
(SISSA-ISAS, Triest)
Thesis: Form Factors and
Correlation Functions
1996-1998: Postdoc
(Max Planck Institute for the Physics
of Complex Systems, Dresden)
1998-2000: Postdoc
(Max Planck Institute of Colloids
and Interfaces, Potsdam)
Since 2000: Group Leader and IMPRS
Coordinator (Max Planck Institute of
Colloids and Interfaces, Potsdam)

Most environments in which life evolves have a stochastic nature. A particularly important element of stochasticity is produced by variations over time of the availability of the resources necessary to growth and reproduction.

For instance, parasites need a host that carries them around in order to get in contact and infect another, healthy, host. If the density of the hosts is very small, the encounters between hosts may be very rare and, from the point of view of the parasite, rather unpredictable. The parasites must therefore adapt to these conditions in order to avoid that all sick hosts die or get immunized before infecting a healthy one. One case study is given by the adaptation of the virus zoster, responsible for varicella, to the dynamics of early human groups [1]. In order to cope with the rare encounters between individuals in sparse populations, this virus has developed a mechanism that allows it to remain latent and inactive within the host after the varicella infection. The later outbreak in form of shingles is a strategy that increases the probability of propagation of the virus and thus enhances its fitness.

Another example is provided by organisms in extreme seasonal environments, where the conditions for growth and reproduction vary strongly from season to season. A much studied case of this kind are plants in deserts. In this environment, the conditions for life are restricted to a few months during winter and the yield, i.e. the number of seeds produced by each plant, may vary very much from season to season so that even zero yields can occur during some seasons. To adapt to such an environment, these species have developed two mechanisms. On the one hand, at the end of the season, the individuals devote all their energy to the production of their seeds and die afterwards. For this reason, they are called annual species. On the other hand, the seeds have a form of dormancy that allows them to germinate only with a certain probability $g<1$ even if the conditions for germination are met at the beginning of the next season. In this way, dormancy is a strategy that mantains a permanent soil seed bank and allows local populations to avoid extinction after seasons without yield [2].

My research has mostly to do with the strategy of seed dormancy. Nevertheless, the methods used, a mixture of stochastic modelling and evolutionary game theory, can be applied to a much broader range of biological problems. In particular, these methods are useful to study evolution under conditions in which the revenue of a certain investment is dependent on external factors which vary strongly and are unpredictable. Presumably, such conditions were also prevalent when the early forms of life had to develop before any kind of homeostasis had emerged.

One important topic of theoretical population biology is to characterize the phenotypes that we would expect on the basis of evolution. In the case of dormant seeds, the phenotype is the fraction g of seeds in the seed bank that should germinate at the beginning of each season.

If the plants cannot predict how good or bad a season will be, they have two simple choices: all seeds germinate, i.e. $g=1$; or all seeds stay dormant, i.e. $g=0$. These two choices are called pure strategies in game theory. To find out whether evolution leads to one of the two pure strategies or to a mixed strategy, i.e. to $0<g<1$, one implements a method called invasibility analysis. The implementation of the method depends on the particular model for the population dynamics. Its main ingredient is to determine whether a small population playing the strategy g' can invade an environment dominated by a large population playing the strategy g. By means of both analytical and numerical techniques [3], this method allows to compute the strategy g^* which survives attempts of invasion by any other strategy. The strategy g^* is then called the evolutionary stable strategy of the system. This means that evolution should lead to the phenotype g^*.

The analysis of how the evolutionary stable strategy g^* depends on other parameters, provides important information about the effect of these parameters on the evolutionary history of the species. In the case of seed dormancy, such parameters are given by the properties of the stochastic variable yield per season.

A particular issue that interested Prof. Katja Tielbörger, a plant ecologist at the University of Tübingen, and myself was the analysis of the evolutionary stable strategy when the seed bank is structured.

An obvious reason for why the seed bank is structured, is that there are seeds of several ages in the soil. If we consider each age as a class, then the seed bank is structured in age classes. From empirical studies on seeds, we know that several mechanical and biochemical processes are at work that have an effect on the germination properties of the seeds. We also know that these effects depend on time and therefore on age. This leads to the expectation that old viable seeds will react differently than younger seeds to optimal germination conditions. In particular, we would intuitively expect that older seeds have a higher germination probability than younger seeds. However, no theoretical studies exist to determine which changes of g we should expect to observe from the point of view of evolution.
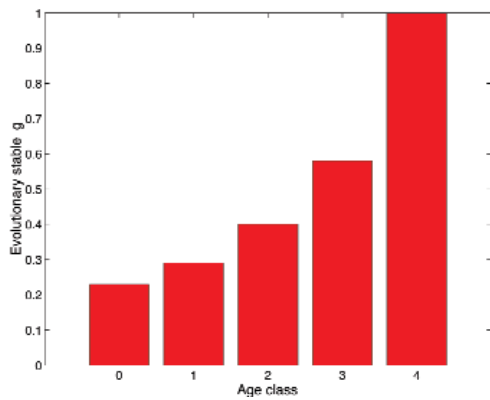
Fig. 1: The evolutionary stable strategy for structured seed banks is that older seeds (right) have higher germination probability than younger seeds (left).

Fig. 2: Seeds from a bad season (blue) have a larger germination probability than seeds from a good season (red).

References:
[1] Stumpf, M.P.H., Laidlaw, Z., and Jansen, V.A.A.: Herpes viruses hedge their bets. PNAS **99**, 15234-15237 (2002).
[2] Bulmer, M.G.: Delayed Germination of Seeds: Cohen's Model Revisited. Theoretical Population Biology **26**, 367-377 (1984).
[3] Valleriani, A.: Algebraic Determination of the Evolutionary Stable Germination Fraction. To appear on Theoretical Population Biology.
[4] Tielbörger, K., Valleriani, A.: Can seeds predict their future? Germination strategies of density-regulated desert annuals. To appear on OIKOS.

We have therefore developed and studied an evolutionary model to follow the evolution of g with the age of the seeds. The main result of the model is that the age-dependent $g*$ will grow with the age of the seeds **(Fig. 1)**. This result is in agreement with the intuitive expectation. It tells also that there must be an adaptation to the mechanical and biochemical mechanisms which influence the germination behaviour.

Another, less obvious structure became clear from several empirical studies. It was noticed that several plant species in several distinct locations produce seeds, which have a low germination probability after a very good season with large yield, and seeds with a large germination probability after a very bad season with small yield **(Fig. 2)**.

Until recently, the theoretical explanation for this empirical observation was based on the idea that the fitness of the plant is increased by decreasing the competition among siblings. This explanation, however, is valid only under particular competition conditions and in the absence of any stochasticity.

We have developed a different evolutionary model where we made the simplifying assumption that there are only two kinds of seasons, good and bad ones. In this way, we could structure the seed bank into two classes: seeds from good seasons and seeds from bad seasons. Our analysis shows that it is evolutionary convenient that seeds from good seasons have a lower germination probability than those from bad seasons.
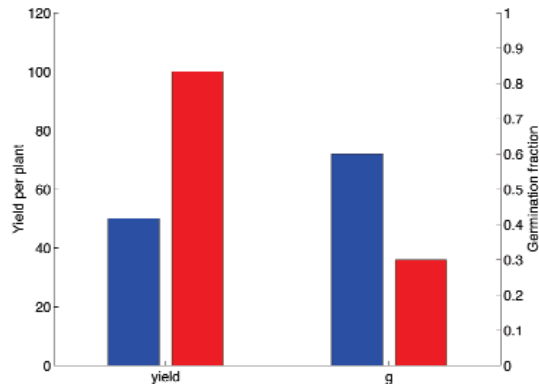
Given the very general assumptions of the model, we concluded that this behaviour should be common to all annual species with permanent soil seed banks **[4]**.

I plan to apply this approach to other systems where evolution through competition between different strategies is believed to play an important role.

Angelo Valleriani
Angelo.Valleriani@mpikg.mpg.de

Advanced Confocal Microscopy

Rumiana Dimova 06.04.1971
1995: Diploma, Chemistry (Sofia University, Bulgaria), Major: Chemical Physics and Theoretical Chemistry, Thesis: Role of the Ionic-Correlation and the Hydration Surface Forces in the Stability of Thin Liquid Films
1997: Second MSc (Sofia University, Bulgaria) Thesis: Interactions between Model Membranes and Micron-Sized Particles
1999: PhD, Physical Chemistry (Bordeaux University, France) Thesis: Hydrodynamical Properties of Model Membranes Studied by Means of Optical Trapping Manipulation of Micron-Sized Particles
2000: Postdoc (Max Planck Institute of Colloids and Interfaces, Potsdam)
Since 2001: Group Leader (Max Planck Institute of Colloids and Interfaces, Potsdam)

The development of laser scanning microscopy has initiated a revolution in the investigation of the spatial structure of microscopic samples. In the last few years confocal microscopes have been improved to accommodate modern techniques like Fluorescence Correlation Spectroscopy (FCS) and Fluorescence Lifetime Image Microscopy (FLIM) thus furnishing the instruments with powerful tools.

FCS is a single molecule method for measuring concentrations and diffusion rates. Only molecules in the confocal volume are excited and detected via the emitted photons. This leads to intensity fluctuations as the molecules cross the confocal volume. FCS evaluates the fluctuations by determining the time dependence of the intensity correlation and by analyzing the time behavior of the fluctuations (see **Fig. 1**).
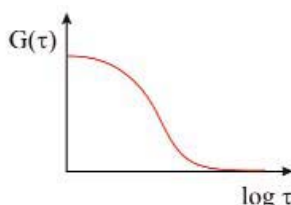

Fig. 1: FCS principle: Only molecules in the confocal volume are excited (left). The time correlation of the intensity spectrum (right) contains the information about the diffusion rates. The illustrations are reproduced from [1].

FLIM is based on time-correlated single photon counting technology. A multiphoton laser is used as excitation source (see **Fig. 2**). The instrument then records the fluorescence spectrum in all pixels of the image, thus allowing for efficient discrimination between different fluorescence markers. This leads to high contrast fluorescence imaging, enhanced depth resolution, less autofluorescence, and less photobleaching outside the focus. In contrast to intensity imagining, FLIM is insensitive to fluctuations in fluorochrome concentration and excitation light intensity.
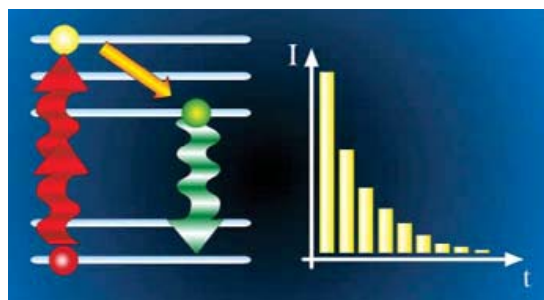

Fig. 2: FLIM principle: After 2-photon excitation (left) the fluorescence decay (right) in each pixel of the image is detected. The illustration is reproduced from [1].

The MPI-KG has recently received additional funding from MPG to install such a confocal microscope equipped with FCS and FLIM. A number of projects involving this microscope will be pursued:

**Domains in Membranes
(Theory Department):**
Giant unilamellar vesicles made of lipid mixtures will be used as a model system to study domain formation in lipid bilayers. The different domains can be visualized by fluorescent probes which preferably partition in one of the phases. Using FCS the local fluidity of the membrane can be probed. As an extension to the confocal microscope setup, we intend to adapt a micropipette system. The micropipettes would allow for manipulation and spatially fixing the vesicle under study. In addition, applying some suction pressure with a pipette induces tension on the aspirated vesicle. We intend to study the effect of membrane tension on the morphology and behavior of the phase separation and domain formation in the lipid bilayer.

**Fusion of Model Membranes
(Theory Department):**
As a model system, we use giant vesicles. Two ways of inducing fusion will be investigated: (i) Membranes functionalized with fusogenic molecules are brought together by means of micropipettes and exposed to a solution of trivalent metal ions. The latter make a fluorescently active coordination complex with fusogenic molecules from opposing bilayers. Thus the membranes are brought together and fuse. (ii) When subjected to short square-wave electric pulses vesicles porate. If two vesicles are close together, they fuse when subjected to the pulse. The fusion of vesicles can be partial consisting of hemifusion where only the external leaflets of the membranes fuse, or complete where the internal volumes of the two vesicles mix. In order to distinguish between the two cases we intend to study fusion on vesicle couples where one of the vesicles is fluorescently labeled and the other is not labeled. Another aspect of this project is related to fusing vesicles of different membrane composition which would lead to constructing membranes with two microdomains. To resolve the dynamics of the fusion process we intend to use FLIM.

Cells on Artificial 3D Scaffolds (Department of Biomaterials):

Here the main purpose of using confocal microscopy is to analyze cells grown on 2D and 3D scaffolds. In order to test different hydroxyapatite materials for their biocompatibility, 3D scaffolds will be seeded with osteoblast-like cells. These cells start forming a tissue-like network from collagen within the holes of the scaffold material. It is an advantage to get a 3D reconstruction from the behavior of the cells in the pores in order to learn how the process of an extracellular matrix formation by osteoblasts develops. The high resolution that a confocal microscope equipped with FLIM allows would also provide the possibility to visualize intracellular structures of the cells to observe changes and reorganization of the cytoskeleton. Depth projection analysis is useful to observe the cells in the porous network. Moreover, the morphology of the cells and the dynamics of their behavior on membranes and stretched membranes can be analyzed.

Microporous Materials for Structural and Electronic Purposes (Department of Colloid Chemistry):

Modern sensing material, solar cells, actuators and catalysts, but also high performance insulating foams and porous construction materials possess a hierarchical pore structure with voids from the nanometer to the micron scale. Confocal microscopy, especially in a "chemical composition mode" (e.g. vibrational mode sensing), is one of the few techniques to characterize texture and structure of such foams (of transparent or thin opaque materials). The requirement for the confocal microscope is maximal resolution (blue laser), specimen penetration, and chemical analysis in the detection.

Selective Permeation of Dyes through Films and Membranes (Department of Interfaces):

A new type of microcapsules with walls of controlled thickness in the nm range and of designed composition (polyelectrolytes, inorganic particles, proteins) has been developed that, in addition, has been coated by a lipid bilayer. Qualitatively, it has been shown that the permeation of macromolecules as well as ions can be switched via pH, salt, light or electromagnetic pulses. The permeation can be followed by time dependent microfluorescence with dye labeled molecules following a bleaching pulse. For an in-depth understanding and control of the properties it is mandatory to systematically vary molecular parameters (size, shape, hydrophilicity, charge) of the permeant, the shell material, and preparation conditions. The experimental requirements are time resolution into the range of seconds, high sensitivity and dynamic range.

Dynamics of Dyes in Polymeric Gels (Department of Interfaces):

Dyes and drugs can be concentration enriched within gels in capsules and then be released by changes of pH, temperature or solvent. The dynamics within these gels is largely unknown. From fluorescence lifetime imaging, we expect to deduce information on the fraction of free dyes and those bound to the matrix. From FCS with polarized emission we expect information on the local dynamics of optical probes. This is of special interest for systems undergoing sol/gel transitions which macroscopically resemble first-order phase transitions, but where the local dynamics remains to be elucidated.

Folding of Polypeptides at Membranes and at Interfaces (Department of Interfaces):

Hydrophobic surfaces have been shown to inhibit the β-sheet formation of the rather small peptide β-Amyloid. Understanding this process is of utmost importance to prohibit diseases like Alzheimer's. The measurement of secondary structure changes is usually based on circular dichroism and Fourier transform infrared spectroscopy but this is very difficult for monolayers. In particular, the kinetics of folding by fluorescence resonance energy transfer will be studied. For this purpose peptides will be labeled by donor and acceptor dyes and particles of hydrophobic and hydrophilic surfaces will be prepared to compare the kinetics.

Emission of Spherical Shells as Optical Resonators (Department of Interfaces):

It is possible to dope polyelectrolyte shells by organic dyes and luminescent semiconductor quantum dots such that the radial position is defined with precision better than 5 nm. This is expected to give rise to so-called "Whispering gallery modes", a narrow optical emission with peaks depending on the precise geometry. The existence of these modes shall be proved by local spectroscopy (in particular FLIM) with individual shells and the properties will be tested in light of recent theories.

R. Dimova
Rumiana.Dimova@mpikg.mpg.de

References:

[1] www.confocal-microscopy.com/ website/sc_llt.nsf